www.sciencemag.org/cgi/content/full/339/6118/429/DC1

Supplementary Materials for

A Radically Configurable Six-State Compound

Jonathan C. Barnes, Albert C. Fahrenbach, Dennis Cao, Scott M. Dyar, Marco Frasconi, Marc A. Giesener, Diego Benítez, Ekaterina Tkatchouk, Oleksandr Chernyashevskyy, Weon Ho Shin, Hao Li, Srinivasan Sampath, Charlotte L. Stern, Amy A. Sarjeant, Karel J. Hartlieb, Zhichang Liu, Raanan Carmieli, Youssry Y. Botros, Jang Wook Choi, Alexandra M. Z. Slawin, John B. Ketterson, Michael R. Wasielewski, William A. Goddard III, J. Fraser Stoddart*

*To whom correspondence should be addressed. E-mail: stoddart@northwestern.edu

Published 25 January 2013, *Science* **339**, 429 (2013)
DOI: 10.1126/science.1228429

This PDF file includes:

Table of Contents

Section A. Materials / General Methods / Instrumentation

All solvents and reaction vessels were degassed for ~30 min by flushing with Ar gas. All reagents were purchased from commercial suppliers (Aldrich or Fisher) and used without further purification. The syntheses of the homo[2]catenane and the preparation of the EPR samples were carried out under an atmosphere of N_2 gas in a glovebox. The compounds **DB**•$2PF_6$ (*38*) and **CBPQT**•$4PF_6$ (*17*) were prepared according to literature procedures. Both analytical and preparative high pressure liquid chromatography (HPLC) were performed on reverse phase-HPLC (RP-HPLC) instruments, using C_{18} columns and a binary solvent system (MeCN and H_2O with 0.1% CF_3CO_2H). Thin layer chromatography (TLC) was performed on silica gel 60 F254 (E. Merck). Column chromatography was carried out on silica gel 60F (Merck 9385, 0.040–0.063 mm). UV-Vis-NIR absorbance spectra were recorded using a UV-3600 Shimadzu spectrophotometer. Nuclear magnetic resonance (NMR) spectra were recorded on a BrukerAvance 600 and Varian P-Inova 500 spectrometers, with working frequencies of 600 and 500 MHz. Chemical shifts are reported in ppm relative to the signals corresponding to the residual non-deuterated solvents (CD_3CN: δ 1.94 ppm). A 1 mM homo[2]catenane sample was prepared in DMF with 100 mM $TBAPF_6$ and placed in a spectroelectrochemical cell with a platinum mesh working electrode, a silver pseudo-reference electrode, and a platinum counter electrode, attached to a Gamry Multipurpose potentiostat. After bulk electrolysis in the glovebox, samples were loaded into quartz 1.4 mm tubes and sealed with a clear ridged UV doming epoxy (IllumaBond 60-7160RCL). All samples were used immediately after preparation. EPR Measurements at X-band (9.5 GHz) were carried out at room temperature using a Bruker Elexsys E580-X EPR spectrometer outfitted with a variable Q dielectric resonator (ER-4118X-MD5-W1). Steady-state CW EPR spectra were measured at X-band using 2 mW microwave power and 2.5 G field modulation at 100 KHz, with a time constant of 5.12 ms and a conversion time of 20.48 ms. Solid state CW EPR was performed on a sample of several monoradical **HC**•$7PF_6$

crystals –which were confirmed by X-ray diffraction – in a quartz 1.4 mm tube in air. Spectra were collected using the same instrument and parameters that were employed for the solution-phase homo[2]catenane samples, including the subtraction of the quartz impurity. SEM imaging was performed on a FEI Quanta 600F sFEG ESEM scanning electron microscope (SEM) at an accelerating electron voltage of 30 kV under high vacuum. The microscopic **HC**•7PF_6 crystal shown (Fig. 3J) in the SEM image was obtained by drop-casting a 0.625 mM CH_3CN solution of the HC onto a silicon wafer, followed by slow-vapor diffusion of *i*Pr_2O onto the surface. The same procedure was used to grow the microscopic crystals of **HC**•6PF_6 (Fig. 3K, CH_3CN) and **HC**•4PF_6 (Fig. 3L, DMF), except the starting solutions were reduced with Zn dust, followed by removal of the dust and drop-casting onto the silicon surface. The magnetic properties of the crystalline monoradical homo[2]catenane and the reference compound **CBPQT**•4PF_6 were measured on pure, dry samples (7.2 mg) using a Quantum Design Superconducting Quantum Interference Device (SQUID) magnetometer (MPMS-5). High-resolution mass spectra were measured on an Agilent 6210 Time of Flight (TOF) LC-MS, using an ESI source, coupled with Agilent 1100 HPLC stack, using direct infusion (0.6mL/min). Cyclic voltammetry (CV) and chronocoulometry (CC) experiments were carried out at room temperature in argon-purged solutions of DMF with a Gamry Multipurpose instrument (Reference 600) interfaced to a PC. All CV and CC experiments were performed using a glassy carbon working electrode (0.071 cm^2). The electrode surface was polished routinely with 0.05 μm alumina-water slurry on a felt surface immediately before use. The counter electrode was a Pt coil and the reference electrode was a Ag/AgCl electrode. The concentration of the sample and supporting electrolyte, tetrabutylammonium hexafluorophosphate ($TBAPF_6$) were 1.0 mM and 0.1 M, respectively. The CV cell was dried in an oven immediately before use, and argon was continually flushed through the cell as it was cooled down to room temperature to avoid condensation of water.

B. Synthetic Protocols

1) Synthesis of HC•7PF$_6$ (HC•6PF$_6$) through DB$^{\bullet+}$ Dimerization

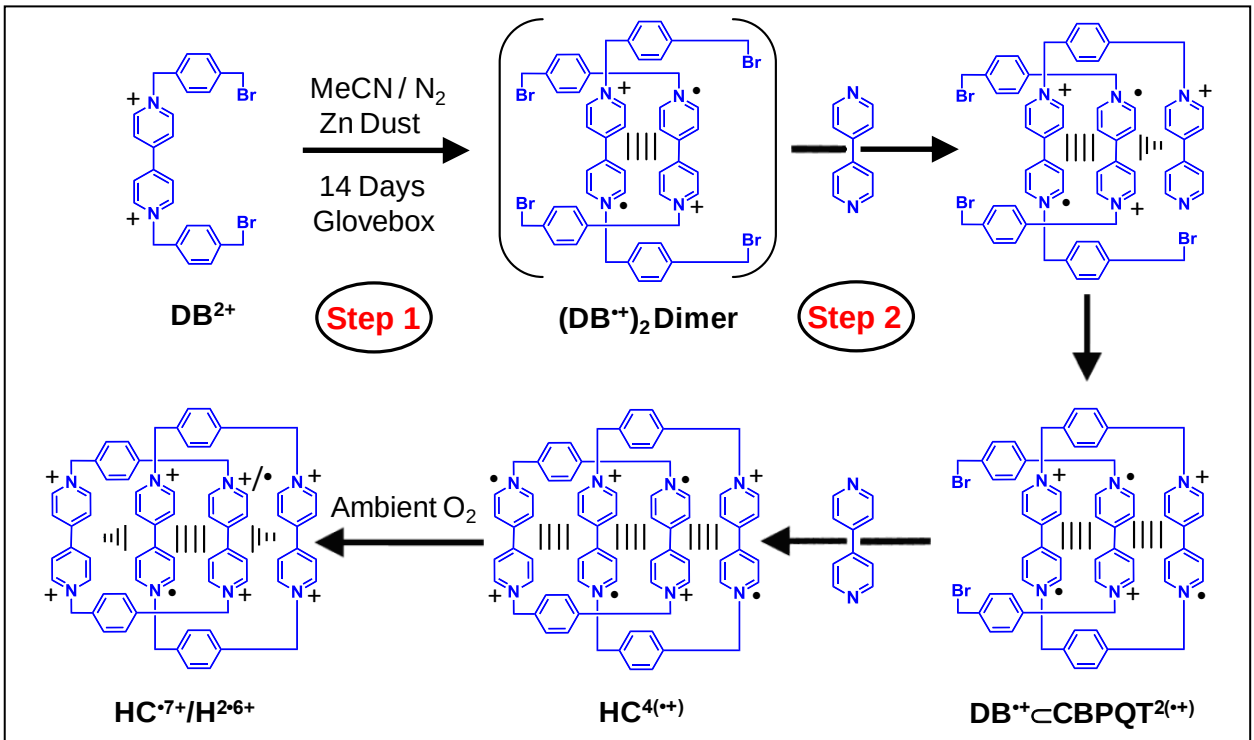

Scheme S1 Synthesis of the monoradical(bisradical) **HC•**7PF$_6$ **(HC•**6PF$_6$**)**. The initial step

HC•7PF$_6$ (HC•6PF$_6$): The following steps (Scheme S1) were carried out in a glovebox under positive N_2 pressure. All solvents and reaction vessels were degassed for ~30 min by flushing with Ar gas. **DB•**2PF$_6$ (122.1 mg, 0.15 mmol) was dissolved in degassed MeCN (15 mL). An excess (3–4 spatula scoops) of Zn dust was added to the reaction mixture which quickly changed (<60 seconds) the color to dark blue. The reaction mixture was then filtered through a 0.45 micron filter disk into a 20 mL scintillation vial, followed by the addition of 4,4'-bipyridine (11.7 mg, 0.075 mmol). After 2 days, the color of the reaction mixture turned purple. The reaction mixture was stirred in the glovebox for 2 weeks and monitored by analytical HPLC. Upon completion of the reaction, an aqueous solution containing NH_4PF_6 (0.1 % w/v) was added outside of the glovebox and the organic layer concentrated, yielding a purple solid suspended in the aqueous layer. Once exposed to ambient conditions, the crude tetradical began to oxidize, ultimately coming to rest at a point somewhere between the bisradical and monoradical states. After filtration, the purple solid was washed with CH_2Cl_2 and the resulting solid was dissolved in a 50:50 H_2O:Me_2SO mixture (5–7 mL; 5% TFA) and purified by reverse-phase high-pressure

liquid chromatography (RP-HPLC) (H_2O / MeCN 0.1% TFA; 0–100 in 70 min). The product fractions were combined, the organic layer was concentrated and NH_4PF_6 was added (0.1% w/v), precipitating out pure **HC**•$7PF_6$ **(HC**•$6PF_6$**)** (fig. S1) as a purple solid (24 mg, 16%); (HRMS-ESI) For **HC**•$7PF_6$, Calcd for $C_{72}H_{64}F_{42}N_8P_7$: *m/z* = 1910.3116 $[M - PF_6]^+$, 882.6734 $[M - 2PF_6]^{2+}$; found: 1910.3139 $[M - PF_6]^+$, 882.6763 $[M - 2PF_6]^{2+}$. For **HC**•$6PF_6$, Calcd for $C_{72}H_{64}F_{36}N_8P_6$: *m/z* = 810.1910 $[M - 2PF_6]^{2+}$, found 810.1927 $[M - 2PF_6]^{2+}$. Because the monoradical is paramagnetic, a strong chemical oxidant (tris(4-bromophenyl)ammoniumyl hexachloroantimonate; "Magic Blue") (*22*), was added in excess to produce the octacationic homo[2]catenane, **HC**•8X, which proved to be "NMR active." ^{1}H NMR (600 MHz, CD_3CN): δ_H 8.99 (d, *J* = 6.4 Hz, 8H), 8.84 (d, *J* = 6.4 Hz, 8H), 8.24 (d, *J* = 8.2 Hz, 8H), 8.11 (d, *J* = 8.2 Hz, 8H), 7.73 (d, *J* = 6.4 Hz, 8H), 6.10 (s, 8H), 5.97 (s, 8H), 4.22 (d, *J* = 6.4 Hz, 8H).

2) Analytical HPLC Analysis of HC•7PF$_6$ (HC•6PF$_6$)

A small aliquot of the purified product **HC**•$7PF_6$ **(HC**•$6PF_6$**)** obtained from preparative RP-HPLC was then treated with a few drops (1% v/v) of concentrated trifluoroacetic acid (TFA) and its purity subsequently confirmed by analytical HPLC (fig. S1).

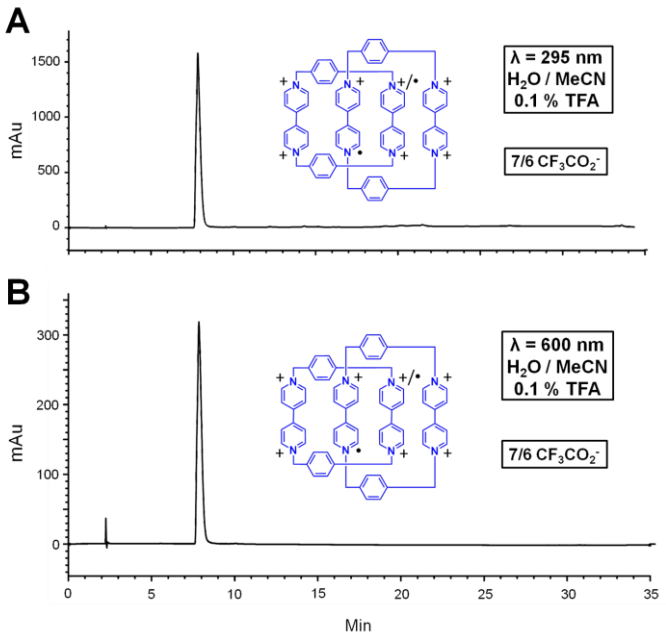

Fig. S1 Analytical RP-HPLC of **HC**•$7CF_3CO_2$ **(HC**•$6CF_3CO_2$**).** (**A**) The photodiode array (PDA) was set at 295 nm. (**B**) The PDA was set at 600 nm.

3) Synthesis of HC•7PF$_6$ (HC•6PF$_6$) through the DB$^{\bullet+}$⊂CBPQT$^{2\bullet+}$ Inclusion Complex

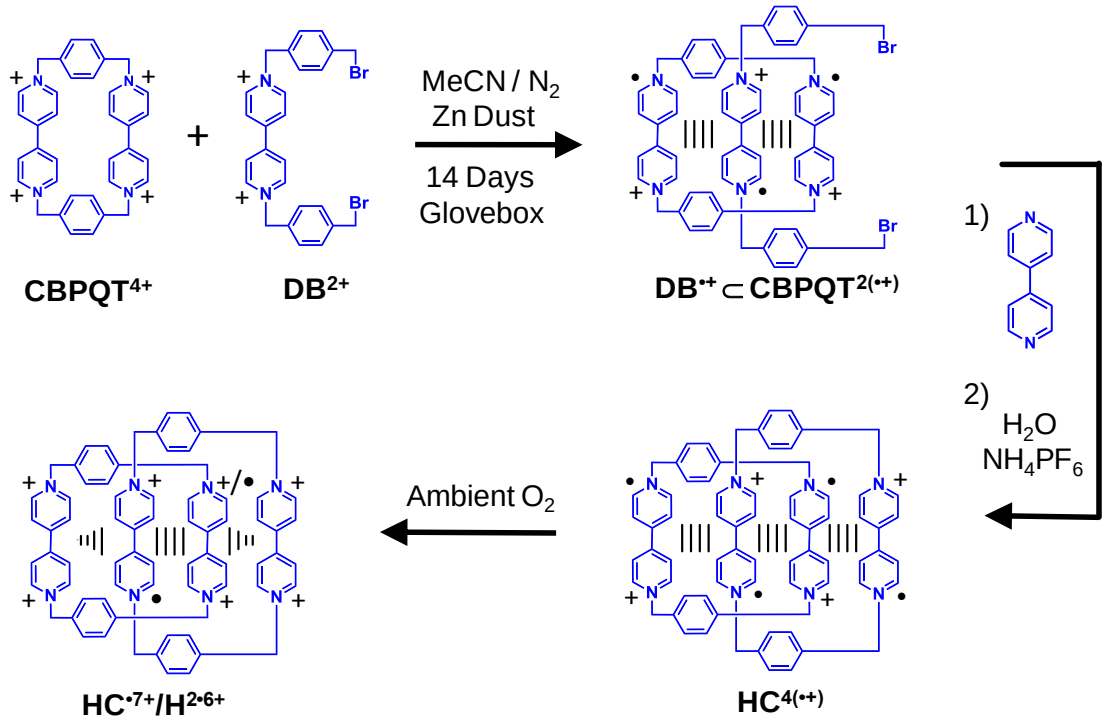

Scheme S2 Synthesis of the monoradical(bisradical) **HC•**7PF$_6$ **(HC•**6PF$_6$**).** The initial step starts immediately with the formation of the trisradical inclusion complex **DB$^{\bullet+}$⊂CBPQT$^{2(\bullet+)}$**.

HC•7PF$_6$ (HC•6PF$_6$): The following steps (Scheme S2) were carried out in a glovebox under positive N_2 pressure. All solvents and reaction vessels were degassed for ~30 min by flushing with Ar gas. **CBPQT**·4PF$_6$ (200 mg, 0.18 mmol) and **DB**·2PF$_6$ (177.6 mg, 0.22 mmol) were dissolved in degassed MeCN (72.7 mL). An excess (3–4 spatula scoops) of Zn dust was added to the reaction mixture, which quickly changed its color to dark blue, followed (<60 sec) by the appearance of a dark purple solution. The reaction mixture was then filtered through a 0.45 micron filter disk into a 250 mL round-bottomed flask, followed by the addition of 4,4'-bipyridine (31.2 mg, 0.22 mmol). The solution was stirred in the glovebox for two weeks and monitored by analytical HPLC. Upon completion of the reaction, an aqueous solution containing NH_4PF_6 (0.1 % w/v) was added outside of the glovebox and the organic layer was concentrated, yielding a purple solid suspended in the aqueous layer. Once exposed to ambient conditions, the crude tetradical began to oxidize, ultimately coming to rest at some point between the bisradical and monoradical states. After filtration, the purple solid was washed with CH_2Cl_2 and the

resultant solid was dissolved in a 50:50 H_2O:Me_2SO mixture (5–7 mL; 5% TFA) and purified by reverse-phase high-pressure liquid chromatography (RP-HPLC) (H_2O / MeCN 0.1% TFA; 0–100 in 70 min). The product fractions were combined, the organic layer was concentrated, and NH_4PF_6 added (0.1% w/v), precipitating out pure **HC**•7PF_6 (**HC**•6PF_6**)** as a purple solid (67 mg, 18%); (HRMS-ESI) For **HC**•7PF_6, Calcd for $C_{72}H_{64}F_{42}N_8P_7$: *m/z* = 1910.3116 $[M - PF_6]^+$, 882.6734 $[M - 2PF_6]^{2+}$; found: 1910.3139 $[M - PF_6]^+$, 882.6763 $[M - 2PF_6]^{2+}$. For **HC**•6PF_6, Calcd for $C_{72}H_{64}F_{36}N_8P_6$: *m/z* = 810.1910 $[M - 2PF_6]^{2+}$, found 810.1927 $[M - 2PF_6]^{2+}$. Because the monoradical is paramagnetic, a strong chemical oxidant (tris(4-bromophenyl)ammoniumyl hexachloroantimonate; "Magic Blue") was added in excess to produce the octacationic homo[2]catenane, **HC**•8X, which proved to be "NMR active." ^{1}H NMR (600 MHz, CD_3CN): δ_H 8.99 (d, *J* = 6.4 Hz, 8H), 8.84 (d, *J* = 6.4 Hz, 8H), 8.24 (d, *J* = 8.2 Hz, 8H), 8.11 (d, *J* = 8.2 Hz, 8H), 7.73 (d, *J* = 6.4 Hz, 8H), 6.10 (s, 8H), 5.97 (s, 8H), 4.22 (d, *J* = 6.4 Hz, 8H).

Section C. Crystallographic Characterization

All crystallographic data are available free of charge from the Cambridge Crystallographic Data Centre via www.ccdc.cam.ac.uk/data_request/cif.

1) HC•6PF_6 Bisradical-Hexacation

a) Methods. Single crystals of **HC**•6PF_6 were grown in a glovebox under positive N_2 by treating a 3.0 mM solution in MeCN with Zn dust, followed by filtration of the purple solution through a 0.45 micron filter disk into a culture tube. Thereafter, slow vapor diffusion of *i*Pr_2O into MeCN solution was allowed to happen over the course of a week. Data were collected at 100 K on a Bruker APEX-II CCD Diffractometer equipped with a CuK_α IμS source and MX optic.

Crystal data for HC•6PF_6. $[C_{72}H_{64}N_8{\cdot}(PF_6)_6]{\cdot}(CH_3CN)_6{\cdot}(H_2O)$. Red block (0.10 x 0.09 x 0.07 mm). Triclinic, *P*–1, *a* = 16.2132(6), *b* = 16.7552(7), *c* = 18.2284(8) Å, α = 84.018(3)º, β = 84.371(3)º, γ = 74.868(3)º, *V* = 4741.1(3) Å^3 , *Z* = 2, *T* = 100(2) K, ρ_{calc} = 1.522 g/cm^3, μ = 2.174 mm^{-1}. Of a total of 16570 reflections which were collected, 16570 were unique (R_{int} = 0.0000, the crystal was twinned and was processed with TWINABS). Final $R_1(F^2 > 2\sigma F^2)$ = 0.1063 and wR_2 = 0.3050. The structure was solved (*39*) by direct methods and expanded using Fourier techniques. Rigid bond restraints (esd 0.01) were imposed on the displacement parameters as well as restraints on similar amplitudes (esd 0.05) separated by less than 1.7 Å on the disordered

PF_6^- counterions. N11 and N14 were restrained (esd 0.01) so that its U_{ij} components approximate to isotropic. CCDC number: 855031.

b) Torsional angles between pyridinium rings. The solid-state structure for $\mathbf{HC}^{2\bullet 6+}$ is illustrated in fig. S2. The torsional angle for each $BIPY^{2+/\bullet+}$ unit is given directly below the structure. The inside $BIPY^{\bullet+}$ units, B and C, possess virtually the same degrees of torsional twisting and are nearly flat (coplanar) considering their torsional angles are approximately 9º – B (esd 1º) and C (esd 1º) – while the outside $BIPY^{2+}$ units, A and D, have larger torsional angles and are asymmetric with respect to each other. This "flattening" effect observed for the inside $BIPY^{\bullet+}$ units results from the delocalization of electron density over each $BIPY^{\bullet+}$ unit. The outside BIPY units possess larger torsional angles and are therefore more buckled, providing evidence that they are more highly charged and are participating very little in radical delocalization, if at all.

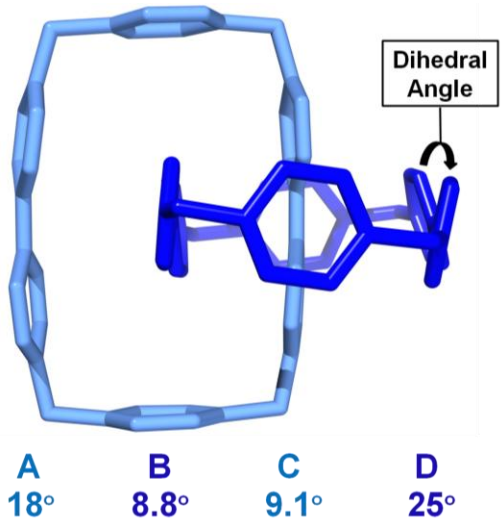

Fig. S2 Solid-state structure of $\mathbf{HC}^{2\bullet 6+}$. The torsional angle of each BIPY is given below the structure. Note the asymmetry in the torsional angles associated with the bisradical state. The product crystallized out with 6 PF_6^- counterions, which have been removed for clarity.

c) Extended superstructure. Further evidence which supports the lack of radical delocalization to involve the outside $BIPY^{2+}$ units can be obtained by inspecting different views of the extended superstructure (fig. S3). From these views, it can be appreciated that there is negligible intermolecular radical-radical interaction, if any, occurring between adjacent homo[2]catenanes. This observation contrasts with the intermolecular interactions which are known to be present in the trisradical $\mathbf{DB}^{\bullet+}\subset\mathbf{CBPQT}^{2(\bullet+)}$ inclusion complex, wherein adjacent $\mathbf{CBPQT}^{2(\bullet+)}$ are all stacked 3.4 Å apart (plane-to-plane) and all of the torsional angles are less than 6(1)º (*vide infra*, fig. S8 and S9).

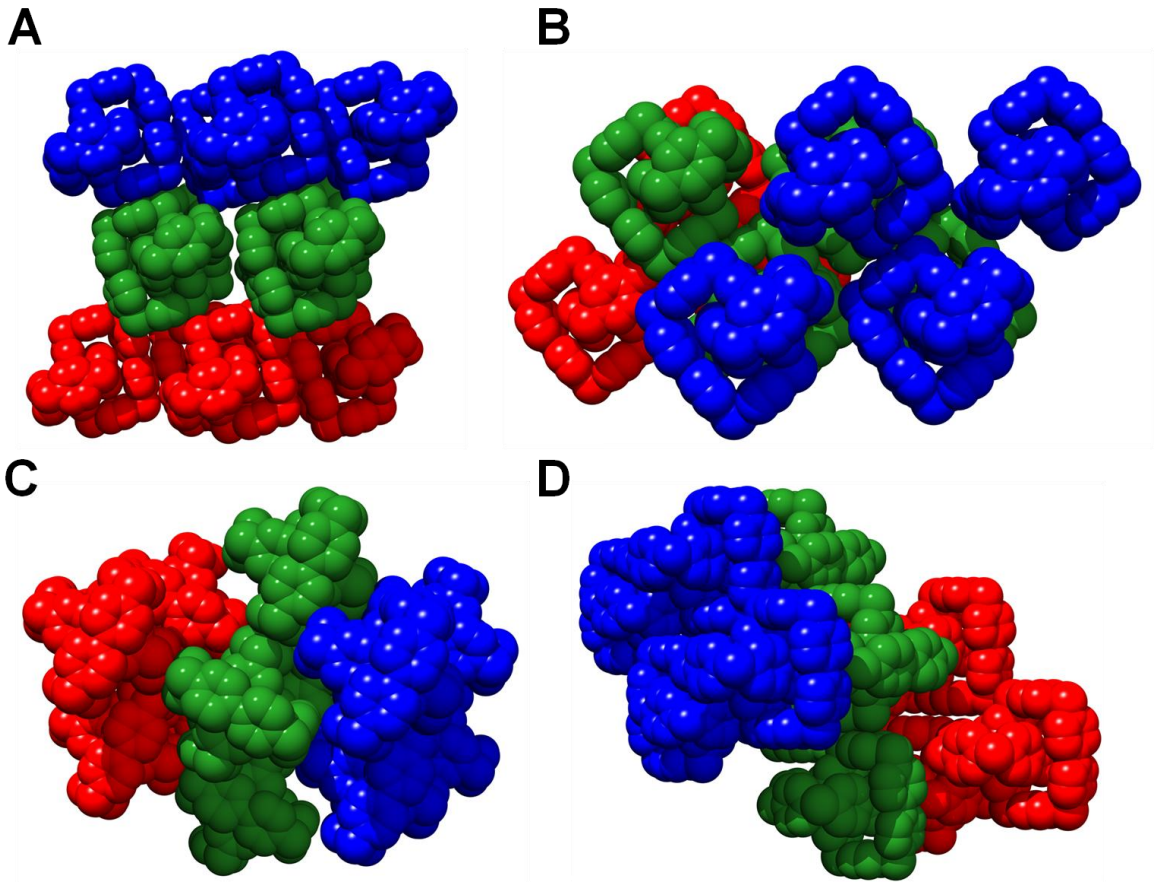

Fig. S3 Space-filling representation of the extended superstructure of **HC**$^{2\bullet 6+}$. The HC units pack into dimers by way of paraphenylene···paraphenylene interactions (closest atomic contact is 3.52 Å) with adjacent dimers having slipped paraphenylene···paraphenylene groups (closest atomic interactions of 3.7 Å and greater). This result provides further support that the outside BIPY^{2+} units participate very little in the delocalization of the radicals. The top two views (**A** and **B**) display the **HC**$^{2\bullet 6+}$ extended structure with the paraphenylene rings facing out of the page, while the bottom two views (**C** and **D**) display the **HC**$^{2\bullet 6+}$ extended structure with the BIPY^{2+} units facing out of the page. The PF_6^- counterions were removed for clarity.

2) HC•7PF$_6$ Monoradical-Heptacation

a) Methods. Single crystals of **HC**•7PF$_6$ were grown on the bench-top by slow vapor diffusion of *i*Pr$_2$O into a 3.0 mM solution in MeCN over the course of a week. All measurements were made at 100 K on a Bruker APEX-II CCD Diffractometer equipped with a CuK$_\alpha$ IμS source and MX optic.

Crystal data for HC•7PF$_6$. $[C_{72}H_{64}N_8{\cdot}(PF_6)_7]{\cdot}(CH_3CN)_6$. Red block (0.21 x 0.16 x 0.08 mm). Monoclinic, C2/c, a = 25.978(2), b = 19.6399(18), c = 18.9216(17) Å, β = 100.204(4)º, V = 9501.4(15) Å^3 , Z = 4, T = 100(2) K, ρ_{calc} = 1.610 g/cm^3, μ = 2.446 mm^{-1}. Of a total of 41796 reflections which were collected, 8393 were unique (R_{int} = 0.0948). Final $R_1(F^2 > 2\sigma F^2)$ = 0.0831 and wR_2 = 0.2295. The structure was solved (*39*) by direct methods and expanded using Fourier techniques. The chemically equivalent, but not symmetry equivalent atoms were restrained so that bond distances and angles were similar. Hydrogen atoms were included in idealized positions, but not refined. CCDC number: 855030.

b) Torsional angles between pyridinium rings. The solid-state structure of **HC**$^{\bullet 7+}$ is shown in fig. S4. The torsional angles are given directly below the homo[2]catenane and there is more similarity between each of the inside $(BIPY_2)^{\bullet 3+}$ units – B (esd 1º) and C (esd 1º) – and between each of the outside $BIPY^{2+}$ units in comparison to the **HC**$^{2\bullet 6+}$ structure, which can be attributed to packing with the PF_6^- counterions. In the case of the **HC**$^{\bullet 7+}$ structure, the inside $(BIPY_2)^{\bullet 3+}$ units also experience a flattening effect with very little buckling between the pyridinium rings in B and C in comparison to the outside $BIPY^{2+}$ units, A and D.

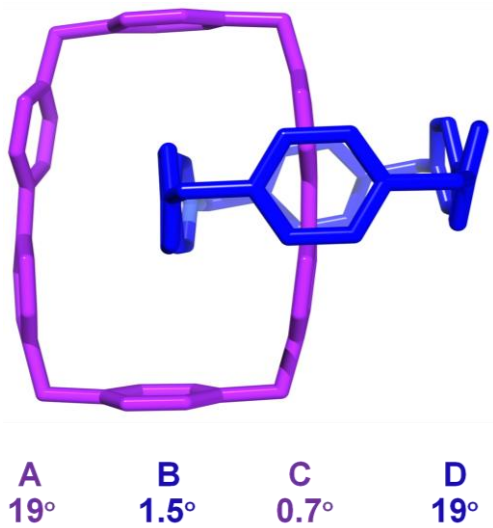

Fig. S4 Solid-state structure of **HC**$^{\bullet 7+}$. The torsional angle of each BIPY is given below the structure. Note the similarity in the torsional angles associated with the monoradical state. The product crystallized out with 7 PF_6^- counterions, which were removed for clarity.

c) Extended superstructure. The extended superstructure of **HC**$^{\bullet 7+}$ is shown in fig. S5 and the absence of intermolecular radical-radical interactions is observed – as was indeed the case in the extended structure of **HC**$^{2\bullet 6+}$– further supporting the view that the outside $BIPY^{2+}$ units participate very little, if at all, in delocalization of the electron density.

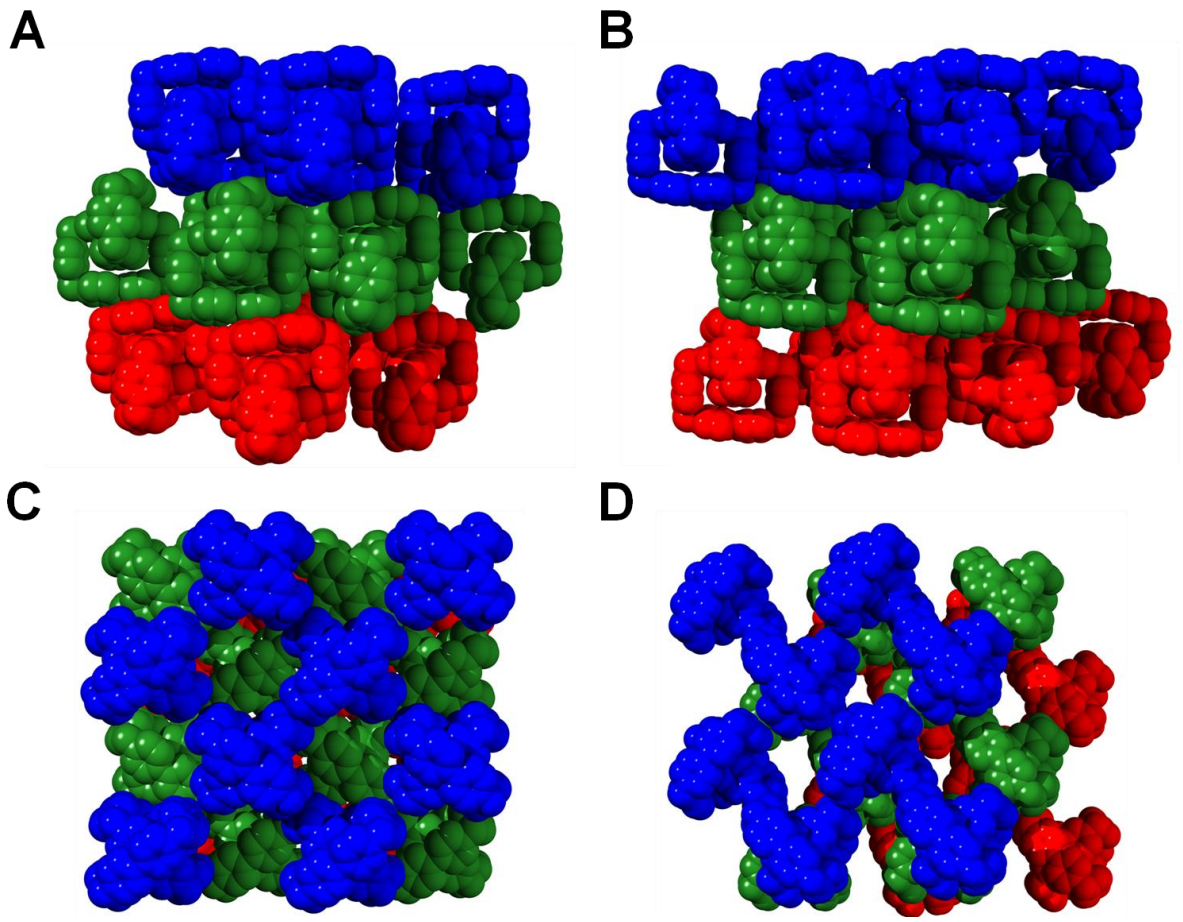

Fig. S5 Space-filling representation of the extended superstructure of **HC**$^{\bullet 7+}$. The packing of the homo[2]catenanes is not ordered by intermolecular radical-radical interactions between the outside BIPY^{2+} units of adjacent molecules. There are significant paraphenylene···paraphenylene interactions (closest C···C distances of 3.6 Å and greater). This result provides further support that the outside BIPY^{2+} units participate very little in the delocalization of the radicals. The top two views (**A** and **B**) display the **HC**$^{\bullet 7+}$ extended structure with the paraphenylene rings facing out of the page, while the bottom two views (**C** and **D**) display the **HC**$^{\bullet 7+}$ extended structure with the BIPY^{2+} units facing out of the page. The PF_6^- counterions were removed for clarity.

3) HC•4PF$_6$ Tetraradical-Tetracation

a) Methods. Single crystals of **HC**•4PF$_6$ were grown in a glovebox under positive N_2 by treating a 3.0 mM solution in DMF with Zn dust, followed by filtration of the brownish-purple solution through a 0.45 micron filter disk into a culture tube. Thereafter, slow vapor diffusion of *i*Pr$_2$O into the DMF solution was allowed to happen during the course of a week. Data were collected

at 99.99 K on a Bruker APEX-II CCD Diffractometer equipped with a CuK_α IμS source and MX optic.

Crystal data for HC•4PF$_6$. $[C_{72}H_{64}N_8\cdot(PF_6)_4]\cdot(C_3H_7NO)_5$. Purple block (0.97 x 0.18 x 0.09 mm). Monoclinic, $P2_1/n$, a = 18.274(4), b = 30.187(6), c = 18.591(4) Å, α = 90.00, β = 91.756(9), γ = 90.00º, V = 10251(4) Å^3 , Z = 4, T = 99.99 K, ρ_{calc} = 1.287 g/cm^3, μ = 1.527 mm^{-1}. Of a total of 130404 reflections which were collected, 17355 were unique (R_{int} = 0.0339). Final $R_1(F^2 > 2\sigma F^2)$ = 0.0414, and wR_2 = 0.1177. The structure was solved (*39*) by direct methods and expanded using Fourier techniques. The chemically equivalent, but not symmetry equivalent atoms were restrained so that bond distances and angles were similar. Hydrogen atoms were included in idealized positions, but not refined. CCDC number: 889233.

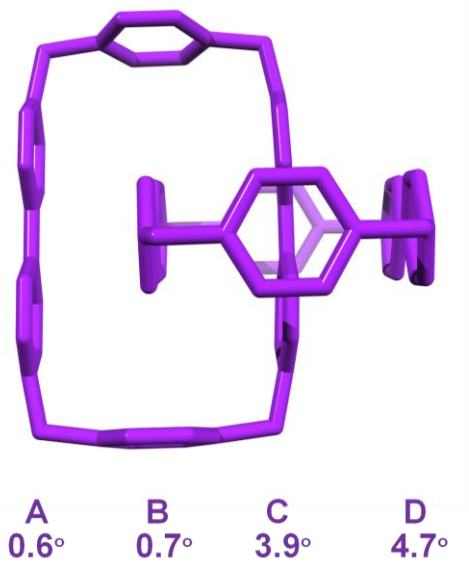

Fig. S6 Solid-state structure of **HC$^{4(\bullet+)}$**. The torsional angle of each BIPY is given below the structure. Note the similarity in the torsional angles associated with the tetraradical state. The product crystallized out with 4 PF_6^- counterions, which were removed for clarity.

b) Torsional angles between pyridinium rings. The solid-state structure of **HC$^{4(\bullet+)}$** is shown in fig. S6. The torsional angles of each BIPY$^{\bullet+}$ unit are given directly below the homo[2]catenane. Note that each angle is below 5º (esd 1º). These angles differ from those observed for the **HC$^{2\bullet6+}$** and **HC$^{\bullet7+}$** structures in that all of the BIPY units experience a flattening effect, an observation which is indicative of tetraradical formation and the complete delocalization of the four radical electrons between the inside and outside BIPY$^{\bullet+}$ units.

c) Extended superstructure. In the extended superstructure (fig. S7) of **HC$^{4(\bullet+)}$** it is evident that the packing of the individual tetraradicals is directed by their intermolecular radical BIPY$^{\bullet+}$···BIPY$^{\bullet+}$ interactions. This observation is in stark contrast to the packing observed for **HC$^{\bullet7+}$** and **HC$^{2\bullet6+}$**, further supporting the view that all of the BIPY units participate in radical delocalization in **HC$^{4(\bullet+)}$**.

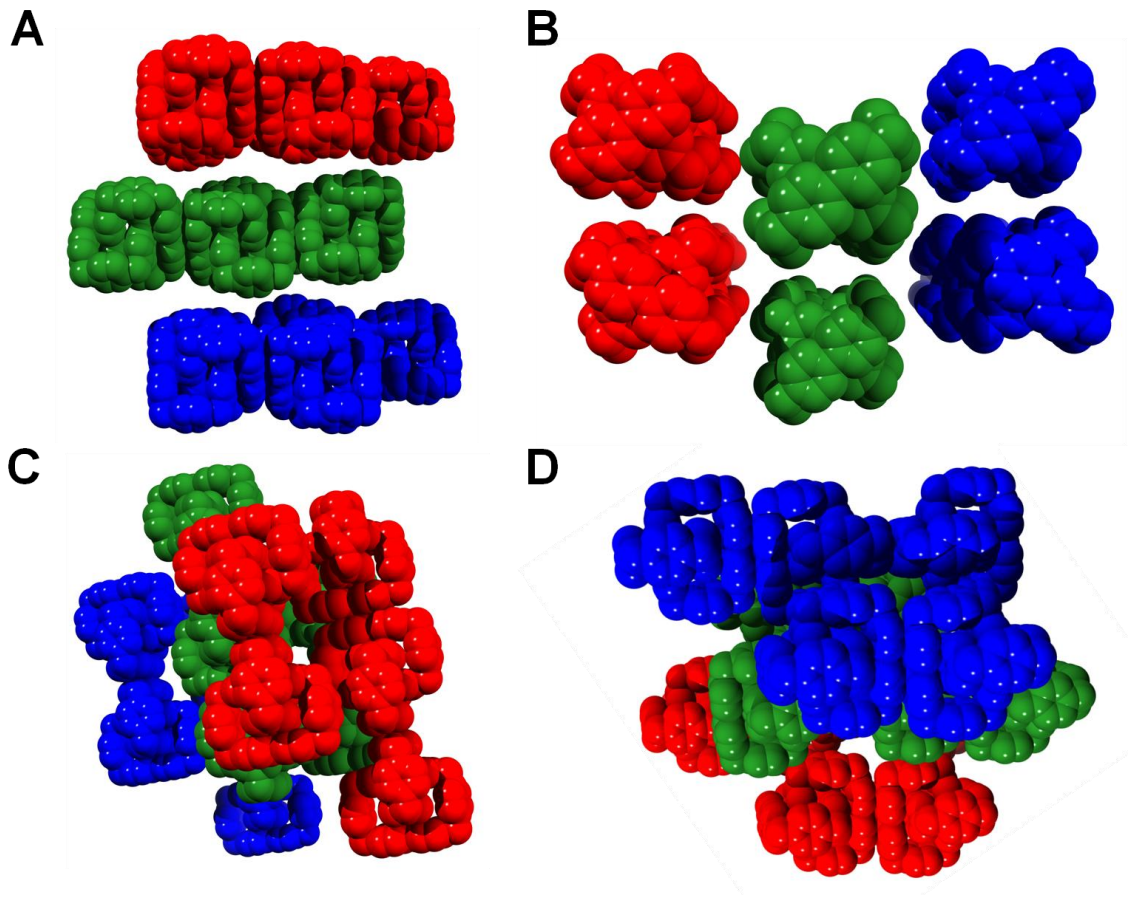

Fig. S7 Space-filling representation of the extended superstructure of **HC$^{4(\bullet+)}$**. The packing of the homo[2]catenanes *is* ordered by intermolecular radical-radical interactions between the outside BIPY$^{\bullet+}$ units of adjacent molecules. There are significant BIPY$^{\bullet+}$··· BIPY$^{\bullet+}$ interactions (closest C···C distances of 3.3 Å and greater). This result provides support for the belief that the outside BIPY$^{\bullet+}$ units participate in the delocalization of the radicals. The top left and bottom two images (**A, C,** and **D**) display the **HC$^{4(\bullet+)}$** extended structure with the paraphenylene rings facing out of the plain of the paper/screen, while the top right view (**B**) displays the **HC$^{4(\bullet+)}$** extended structure with the BIPY$^{\bullet+}$ units facing out of the page. The PF_6^- counterions were removed for clarity.

3) DB⊂CBPQT•3PF$_6$ Trisradical Intermediate

a) Methods. Single crystals of the **DB⊂CBPQT•**3PF$_6$ inclusion complex were grown in a glovebox under positive N_2 by preparation of a 2.5 mM **CBPQT•**4PF$_6$ / 3.0 mM **DB•**2PF$_6$ solution in MeCN followed by the addition of an excess of Zn dust. The reduced, purple solution was then filtered through a 0.45 micron filter disk into a culture tube. Finally, slow vapor diffusion of *i*Pr$_2$O into the MeCN solution was allowed to happen over the course of a week.

All measurements were made at 100 K on a Bruker APEX-II CCD Diffractometer equipped with a CuK_α IμS source and MX optic.

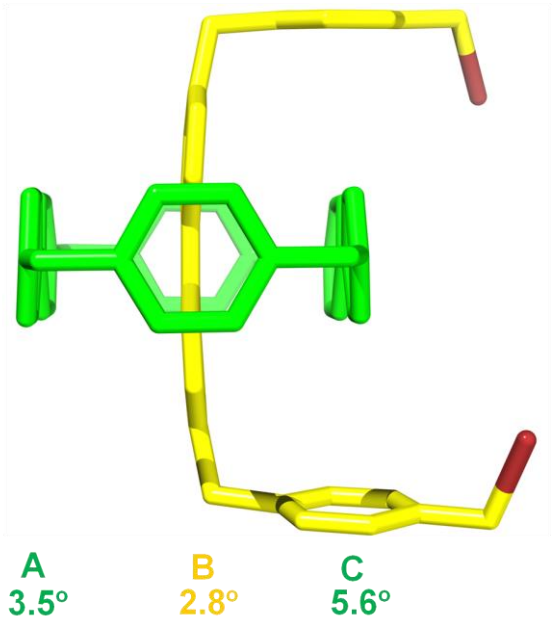

Fig. S8 Solid-state structure of **DB$^{\bullet+}$⊂CBPQT$^{2(\bullet+)}$.** The torsional angle of each BIPY$^{\bullet+}$ unit is given below the structure. Note the small value of the torsional angles in this trisradical state. The product crystallized out with 3 PF_6^- counterions, which have been removed for clarity.

Crystal data for DB⊂CBPQT•3PF$_6$. $C_{62}H_{56}Br_2N_6{\cdot}(PF_6)_3$ Black cube (0.21 × 0.06 × 0.05 mm). Orthorombic *Pccn*, a = 20.9361(16), b = 14.8826(12), c = 19.4989(13) Å, V = 6075.5(8) Å^3 , Z = 4, T = 100(2) K, ρ_{calc} = 1.618 g/cm^3, μ = 3.348 mm^{-1}. Of a total of 26616 reflections which were collected, 5113 were unique (R_{int} = 0.0977). Final $R_1(F^2 > 2\sigma F^2)$ = 0.0839 and wR_2 = 0.2177. The structure was solved (*39*) by direct methods and expanded using Fourier techniques. No disorder was observed in the sample; no restraints were used in the refinement. CCDC number: 855032.

b) Torsional angles between the pyridinium rings. Fig. S8 shows the solid-state structure of the **DB$^{\bullet+}$⊂CBPQT$^{2(\bullet+)}$** complex. The torsional angle for each BIPY$^{\bullet+}$ unit is given directly below the structure. All of the BIPY$^{\bullet+}$ units are in their radical cation form, and are therefore essentially flat (coplanar) in the sense that their respective torsional angles are less than 6(1)º. Again, this flattening effect is a result of delocalization of electron density over each BIPY$^{\bullet+}$ unit.

c) Extended superstructure. Fig. S9 shows the extended superstructure of **DB$^{\bullet+}$⊂CBPQT$^{2(\bullet+)}$**. In this example, all of the BIPY units are reduced to BIPY$^{\bullet+}$ radical cations and therefore strong intermolecular radical-radical interactions are imposed on the superstructure. These interactions lead to uniform stacking of all of the BIPY$^{\bullet+}$ units, which are separated by a plane-to-plane distance of 3.4 Å. Based on this evidence, a comparison can be made with the **HC$^{\bullet7+}$** and **HC$^{2\bullet6+}$**

superstructures, wherein there is no evidence for intermolecular radical-radical interactions and no uniform stacking occurs either between the molecules' doubly charged outer $BIPY^{2+}$ units. This result further supports the claim that $BIPY^{\bullet+}$ units can be identified from $BIPY^{2+}$ units by measuring the torsional angle between the pyridinium rings of each BIPY unit and the intermolecular distances between each $BIPY^{\bullet+}$ unit.

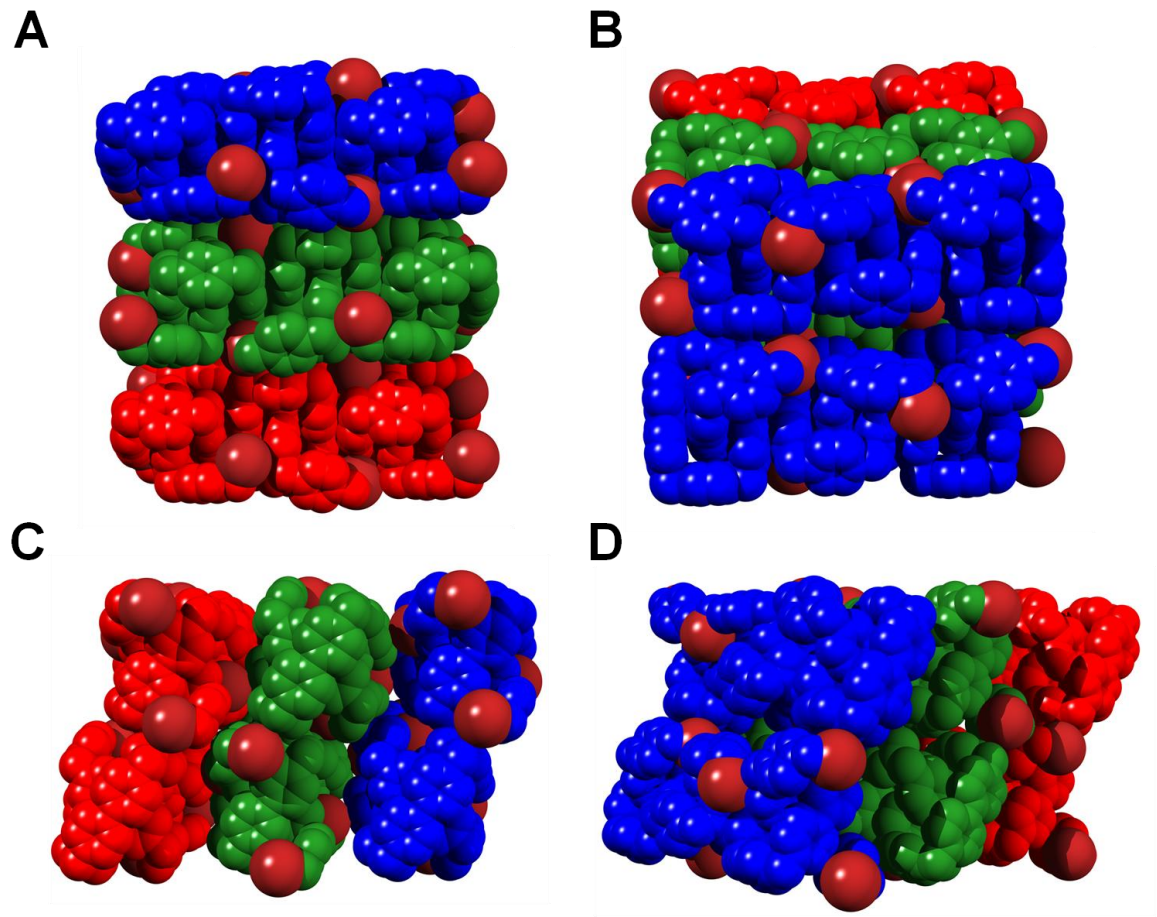

Fig. S9 Extended superstructure of **DB$^{\bullet+}$⊂CBPQT$^{2(\bullet+)}$**. Packing of the trisradical intermediate is ordered by intermolecular radical-radical interactions between the $BIPY^{\bullet+}$ units of **CBPQT$^{2\bullet+}$**. This result further supports the claim that $BIPY^{\bullet+}$ units can be identified from $BIPY^{2+}$ units by measuring the torsional angle between the pyridinium rings of each $BIPY^{2+/\bullet+}$ unit as well as the intermolecular distances between each $BIPY^{2+/\bullet+}$ unit. The top two views (**A** and **B**) display the **DB$^{\bullet+}$⊂CBPQT$^{2(\bullet+)}$** extended structure with the paraphenylene rings facing out of the page, while the bottom two views (**C** and **D**) display the **DB$^{\bullet+}$⊂CBPQT$^{2(\bullet+)}$** extended structure with the $BIPY^{\bullet+}$ units facing out of the page. The PF_6^- counterions were removed for clarity.

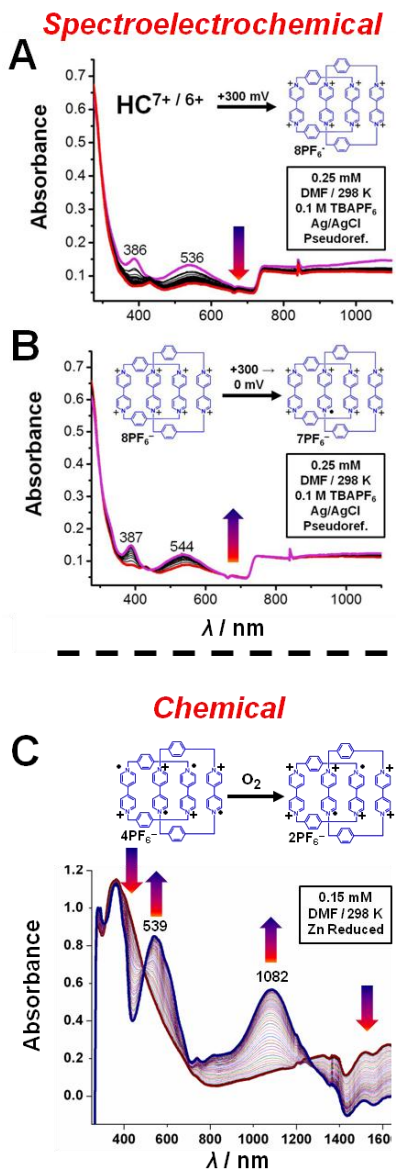

Fig. S10 Spectroelectrochemistry of a 0.25 mM solution of the homo[2]catenane in DMF vs. a Ag/AgCl pseudoreference. (**A**) The starting state UV/Vis/NIR spectrum displays a NIR absorbance at 1075 nm signifying the presence of the bisradical $\mathbf{HC}^{2\bullet 6+}$. (**B**) The monoradical $\mathbf{HC}^{\bullet 7+}$ lacks an absorption band in the NIR. (**C**) The UV/Vis/NIR spectrum of a Zn-reduced 0.15 mM DMF solution demonstrates the conversion of tetraradical $\mathbf{HC}^{4\bullet +}$ to the bisradical $\mathbf{HC}^{2\bullet 6+}$ after exposure to air.

Section D. Spectroscopic and Electrochemical Characterizations

1) Redox-states of the Homo[2]catenane

a) UV/Vis/NIR Optical absorption spectra. Spectroelectrochemistry was performed (fig. S10) on a solution of the homo[2]catenane in DMF in order to evaluate the optical properties of the radical redox states. A UV/Vis spectrum of the homo[2]catenane in DMF after exposure to ambient O_2 reveals (fig. S10A, purple trace) absorption bands centered on 386 and 536 nm, as well as a broad band in the near IR. In order to explain the presence of the absorption band in the near IR, we hypothesize that the homo[2]catenane exists as a dynamic mixture of $\mathbf{HC}^{\bullet 7+}$ and $\mathbf{HC}^{2\bullet 6+}$. Application of a +300 mV voltage results in gradual disappearance of these bands into the baseline, a trend which is consistent with the generation of the $\mathbf{HC}^{8+}$ octacation. Fig. S10B shows the resulting spectra after application of 0 mV directly following application of the +300 mV potential. Absorption bands centered on 387 and 544 nm result, with virtually no band in the near IR – an observation which is consistent with formation of the monoradical heptacation $\mathbf{HC}^{\bullet 7+}$ as the predominant species in solution. When a 0.15 mM DMF solution of the HC was reduced in

an Ar-filled glovebox for 15–20 min with Zn dust, however, the color of the solution became brownish-purple as a consequence of the generation of the tetraradical tetracation **HC**$^{4(\bullet+)}$, which was characterized by UV/Vis/NIR absorption spectroscopy (fig. S10C, brown trace) in a teflon-capped UV/Vis cell (l = 1 cm) by the presence of a broad band in the NIR centered on 1600 nm. Consecutive spectra of the sample were recorded as **HC**$^{4(\bullet+)}$ oxidized slowly under ambient conditions, leading to a decrease in the NIR band at 1600 nm and the growth of two new bands centered on 539 nm and 1082 nm (fig. S10C, blue trace). Additionally, an isosbestic point is observed at 490 nm, indicating the conversion from the tetraradical **HC**$^{4(\bullet+)}$ to the bisradical **HC**$^{2\bullet 6+}$ upon oxidation. The large Gaussian curve at 1082 nm in the spectrum (fig. S10C) of **HC**$^{2\bullet 6+}$ is an indication of mixed-valence behavior within the bisradical.

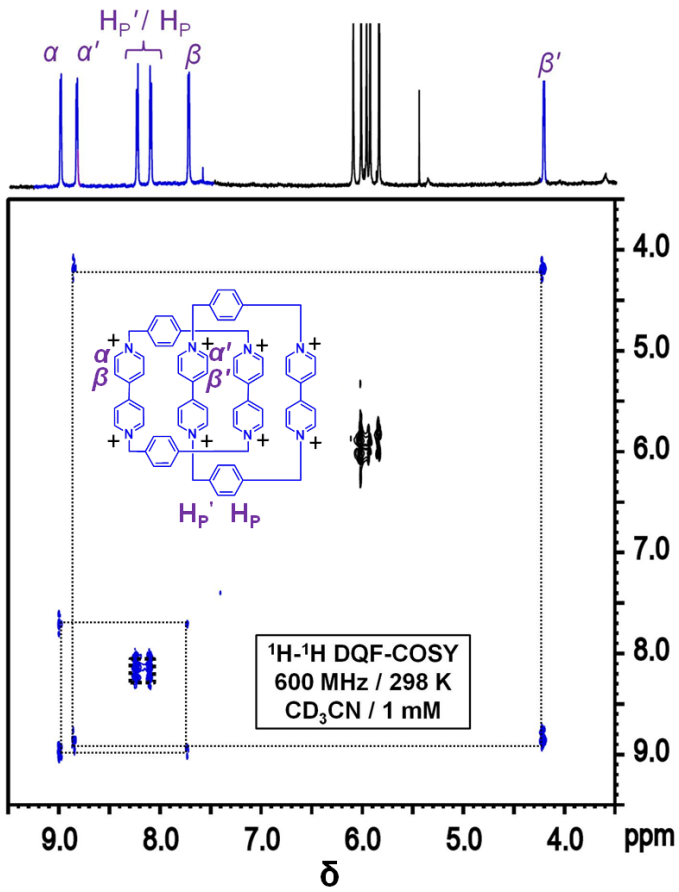

Fig. S11 ^{1}H-^{1}H COSY spectrum of **HC•**8X. The coupling between the outside α and β BIPY^{2+} protons, as well as the coupling between the inside α' and β' BIPY^{2+} protons is shown. It is important to note the dramatic upfield shift of the β' protons is a result of shielding [C-H···π] interactions.

*b) ^{1}H NMR spectroscopic analysis of **HC•**8X.* Attempts to record ^{1}H NMR spectra of the bench-top homo[2]catenane sample in CD_3CN at room temperature revealed no sharp resonance at all for any of the aromatic protons, presumably because of the presence of the paramagnetic species. This situation was resolved by adding an excess of the strong chemical oxidant tris(4-bromophenyl)ammoniumyl hexachloroantimonate ("Magic Blue") (*22*) to the sample in the NMR tube. On oxidation of the homo[2]catenane to diamagnetic **HC**$^{8+}$, the ^{1}H NMR spectrum

(fig. S11) revealed the presence of eight signals (two sets of four) for protons associated with inside and outside $BIPY^{2+}$ units on the two equivalent $CBPQT^{4+}$ rings, implying the absence of circumrotation of the rings with respect to each other at room temperature on the ^1H NMR timescale. Moreover, the resonances for the inside α' and β' protons are shifted upfield, more significantly for the β' protons which resonate at 4.22 ppm, presumably as a consequence of their lying in the shielding zone of the juxtapositioned paraphenylene rings. A ^1H-^1H DQF-COSY spectrum (fig. S11) recorded from a CD_3CN solution of the fully oxidized $\mathbf{HC}^{8+}$ provided confirmation of the proton assignments of the resonances observed in the 1D spectrum. Correlation crosspeaks observed between the resonances, ascribed to the α / β, α′ / β′ and H_P and H_P', corroborate these proton assignments.

c) Electron paramagnetic resonance (EPR) analysis. Fig. S12 shows a solid-state CW EPR spectrum for the **HC**•$7PF_6$ single-crystals, after they were grown on the bench-top and used to

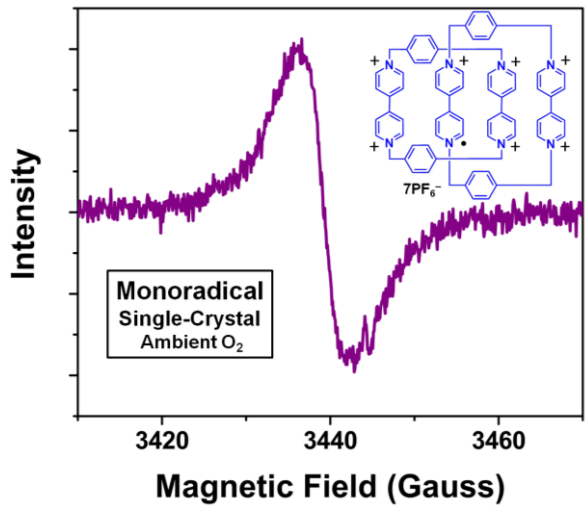

Fig. S12 Solid-state CW EPR of **HC**•$7PF_6$ single-crystals**.** CW EPR analysis on the single-crystals that were used to obtain the X-ray diffraction data for the monoradical **HC•7PF$_6$**. This data supports the crystallographic assignment and it confirms the starting state (bench-top) material is paramagnetic in the solid-state.

obtain the structure shown in fig. S4. This result provides confirmation that the starting state (bench-top) material is paramagnetic in the solid-state for the monoradical heptacation, and supports the crystallographic assignment of the 7+ redox state.

d) Magnetic susceptibility analysis of ***HC•7PF$_6$***. In order to evaluate the radical properties in a bulk sample of **HC•**7PF$_6$, 7.2 mg of the crystalline monoradical redox state were grown on the bench top – by way of slow-vapor diffusion of *i*Pr$_2$O into a 3 mM MeCN solution of ***HC•7PF$_6$*** ***(HC•6PF$_6$)*** – and the single crystals were transferred to a capsule for analysis (fig. S13–S14) in a SQUID magnetometer. Based on the crystallographic data, this crystallization process should provide exclusively the monoradical redox state. The magnetization (*M*) versus temperature (*T*)

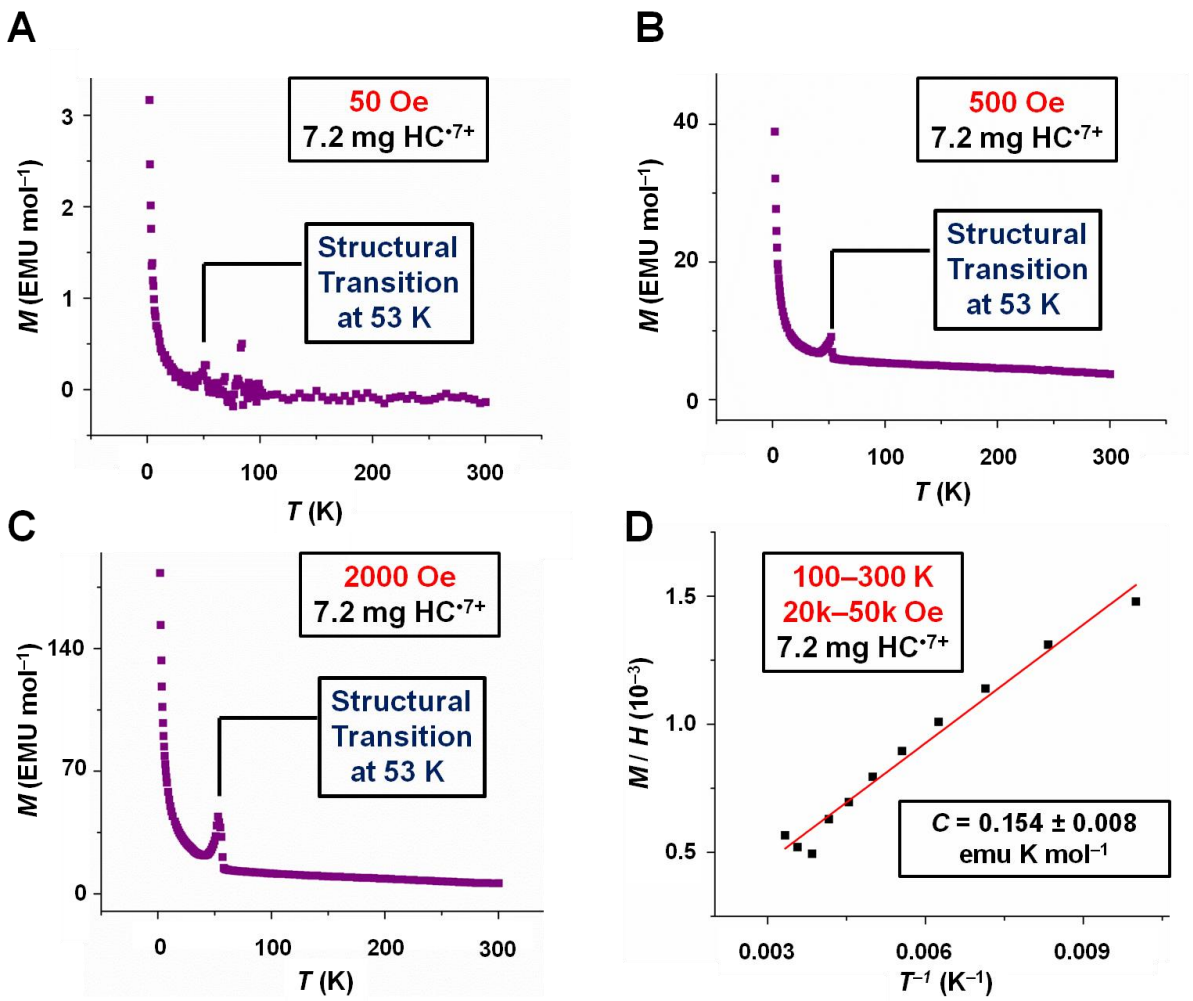

Fig. S13 Magnetic susceptibility analysis of **HC•**7PF$_6$. The molar magnetic susceptibility (*M*) of **HC•**7PF$_6$ versus temperature (*T*) is displayed at three applied fields – 50 (**A**), 500 (**B**), and 2000 Oe (**C**) – for a 7.2 mg crystalline monoradical sample. Note the small spike in magnetization at approx. 53 K, which is attributable to either a structural change of the HC, or some contribution from molecular oxygen at that temperature. A plot of *M/H* vs. T^{-1} is displayed (**D**) for 11 measurements carried out on the same monoradical sample over a high-field (20k–50k Oe) and high temperature (100–300 K) range wherein the Curie constant (*C*) for the bulk HC sample has been obtained directly from the slope of the fitted line (Adj. R^2 = 0.976).

of **HC**•7PF_6 is displayed in fig. S13 at three different applied fields – 50 (A), 500 (B), and 2000 Oe (C). In each case, the *M*(*T*) curve drops suddenly at the start of the measurement at 1.98 K and then declines gradually to zero magnetization at room temperature (300 K). This type of behavior is in agreement with a paramagnet in the sense that the unpaired spins align at a very low temperature, while the magnetization decreases as a function of temperature ($M \propto T^{-1}$). It is important to note the feature at 53 K, where there appears to be a small temporary spike in the magnetization, which can most likely be attributed to either a structural change in the HC, or possibly some contribution from molecular oxygen (O_2) at that temperature. This feature was present at all of the applied fields and in every magnetic experiment of the monoradical crystals repeated thereafter, where different field-dependent values for the Curie constant were obtained. Since the nature of this structure transition requires further investigation, we have confined the analysis of the Curie law contribution to temperatures safely above the transition temperature. At higher fields, the magnetization of the monoradical crystalline sample can be represented by three contributions: i) an overall diamagnetic response (χ_D), ii) a paramagnetic Curie law contribution ($C \cdot T^{-1}$), and iii) a small hysteretic component (M_S) which saturates at low fields and the origin of which is not fully understood. For fields above this saturation point, the following form (*eq. S1*) gives a good representation of the three contributions:

$$M(T,H) = \chi_D H + \frac{C}{T} H + M_S \qquad \textit{Eq. S1}$$

where *H* is the applied field, *T* is the temperature expressed in K, and *M* is the magnetization. A plot of *M/H* vs. T^{-1} is displayed (fig. S13D) for 11 data points of the same monoradical sample. The data was collected at high-field (20k–50k Oe) and in a stepwise manner at fixed temperatures over the range between 100–300 K, from whence the Curie constant (C = 0.154 emu K mol^{-1}) for the bulk HC sample is obtained directly from the slope of the fitted line. The reliability of the fitted (negative) diamagnetic susceptibility χ_D was assessed by comparing it with the value obtained for the control compound **CBPQT**•4PF_6, which demonstrates no hysteresis and the susceptibility was found accurately to be temperature independent, i.e. $\chi_D^{\boldsymbol{CBPQT}\bullet 4PF6} = -1.67 \text{ x } 10^{-8}$ emu mol^{-1} versus $\chi_D^{\boldsymbol{HC}\bullet \boldsymbol{7PF6}} = -2.24 \text{ x } 10^{-8}$ emu mol^{-1}. An alternative analysis involves quite simply subtracting the diamagnetic contribution of the control from that of **HC**•7PF_6. The value of the experimentally determined Curie constant can then be compared with the predicted value (0.375 emu K mol^{-1}) for an organic radical with non-

interacting ions using the following equation for a two-level system and converting between SI and cgs units:

$$C = \frac{N_A}{3k_B}\mu_{eff}^2 \qquad \textit{Eq. S2}$$

where N_A is avogadro's number (6.022 x 10^{23} mol^{-1}), k_B is Boltzmann's constant (1.3807 x 10^{-23} J T^{-1}), and μ_{eff} is the magnetic moment of the compound in question, which can also be represented by

$$\mu_{eff} = g[S(S+1)]^{1/2}\mu_B = [n(n+2)]^{1/2}\mu_B \qquad \textit{Eq. S3}$$

where μ_B is the Bohr magneton (9.274 x 10^{-24} J T^{-1}), $S = \pm\frac{1}{2}$, n is the number of unpaired electrons per ion, and a spin-only approximation of the magnetic moment is assumed. Using the experimentally-determined average Curie constant (C_{exp} = 0.154 emu K mol^{-1}), the radical concentration of the bulk **HC**$^{\bullet 7+}$ crystalline material can be calculated as follows:

$$Conc. = \frac{C_{exp}}{C_{lim}}\ x\ 100\% = \frac{0.154}{0.375}\ x\ 100\% = 41\% \qquad \textit{Eq. S4}$$

This result means the overall radical content of the monoradical crystals is approximately 41% of the expected value. We suggest that this lower value could very well be a consequence of a lack of long-term stability of the monoradical in the solid state.

An examination of the compound's magnetization (M) as the field (H) is varied at 10, 50, 100, and 300 K (fig. S14) affirms the paramagnetic behavior of **HC**$^{\bullet 7+}$ in the high-field regions (i.e., 20,000 – 50,000 Oe) where it is observed that the slope decreases as the temperature is increased (insets of fig. S14A–D) as a result of the paramagnetic temperature dependence. In the low-field regions – inside of ± 3000 Oe – a trend exists where an asymptotic step starts to develop at 50 K and becomes more prominent in the higher temperature range where the diamagnetic component is usually higher. This intrinsic trend is not yet fully understood and it appears the true paramagnetic nature of **HC**$^{\bullet 7+}$ can be gleaned from the high-field magnetic data.

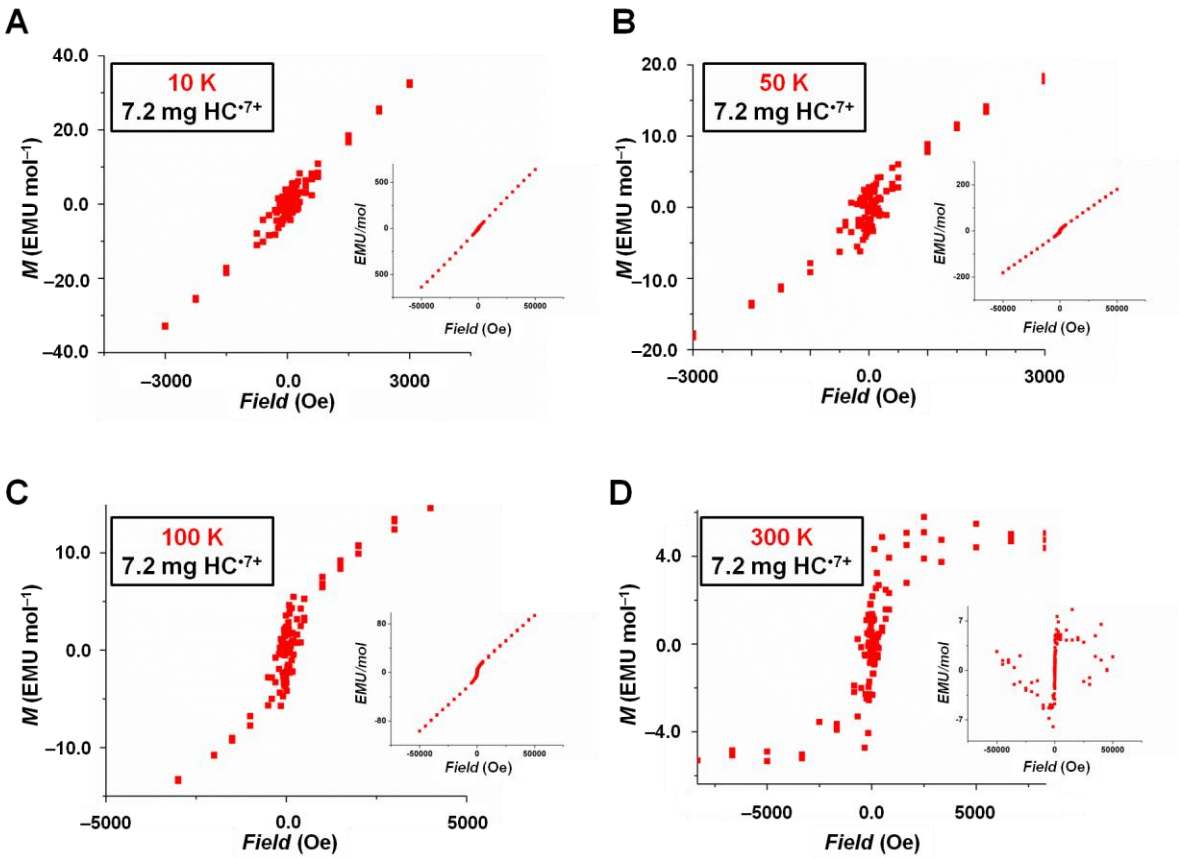

Fig. S14 Magnetization (*M*; EMU mol^{-1}) versus *Field* (Oe) analysis of **HC•**7PF$_6$. The magnetic response of **HC•**7PF$_6$ was measured as the applied magnetic field was varied at 10 (**A**), 50 (**B**), 100 (**C**), and 300 K (**D**). The general paramagnetic trend of decreased magnetization in the high-field region (i.e., 20,000 – 50,000 Oe) is observed as the temperature is increased to 300 K, as evidenced by the smaller and smaller slopes at higher temperatures. The asymptotic step in the low-field region becomes more prominent at higher temperatures where the paramagnetic contribution typically falls completely off. This low-field ordering is not yet fully understood.

In the case of each of the magnetization plots displayed in fig. S14, the diamagnetism was corrected by carrying out the same set of magnetic susceptibility experiments for the control compound **CBPQT•**4PF$_6$, which possesses no radical electrons and mimics closely one of the ring components of **HC**$^{\bullet 7+}$, as if the HC were completely oxidized. Using an identical amount of material (7.2 mg), the magnetization of **CBPQT•**4PF$_6$ was plotted versus an applied field and versus temperature (fig. S15A–D and S16A–C, respectively). The results of these experiments show that the control compound exhibits no paramagnetism and displays only diamagnetic behavior, i.e., negative slopes in fig. S15 and mostly flat lines in fig. S16. These data were used

to perform a point-for-point correction of the diamagnetic contribution of the data shown in fig. S14 by subtracting the EMU values obtained for the diamagnetic control (**CBPQT**•$4PF_6$) from those obtained for the magnetic sample (**HC**$^{\bullet 7+}$).

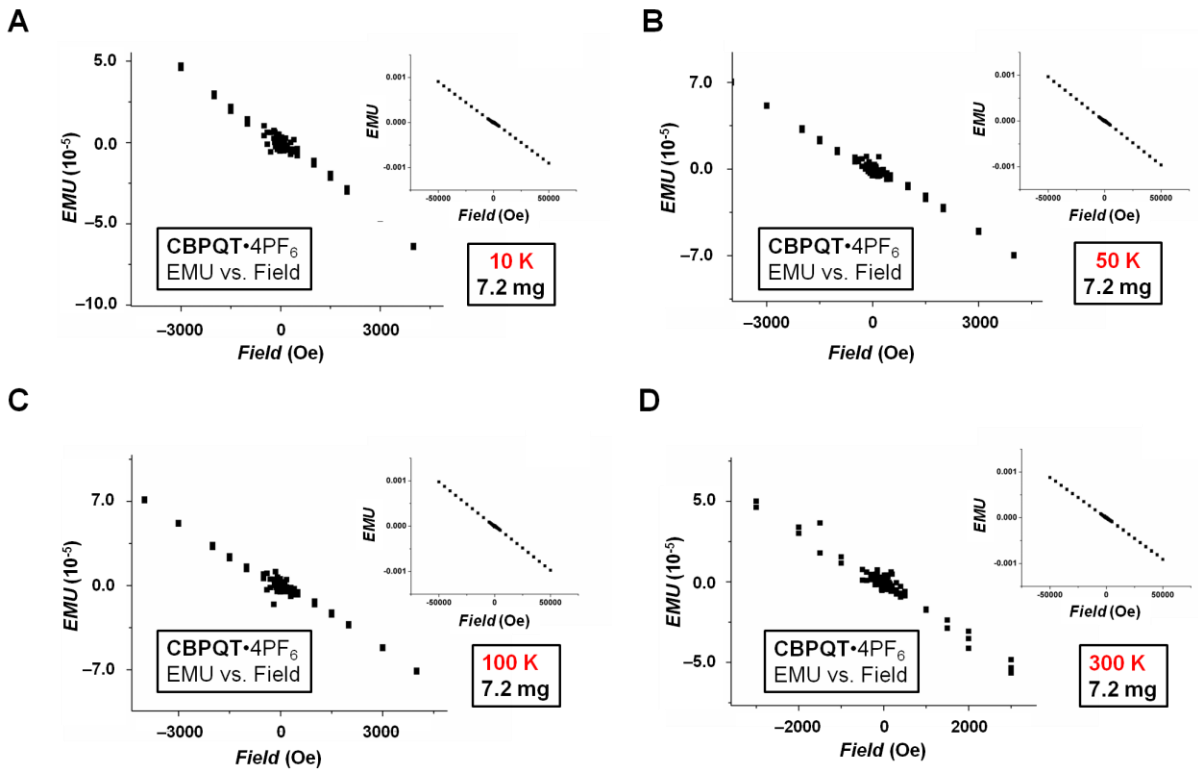

Fig. S15 Magnetization (*EMU*) versus *Field* (Oe) plots of the control compound **CBPQT**•$4PF_6$. The magnetic response of **CBPQT**•$4PF_6$ was measured while the applied magnetic field was varied at 10 (**A**), 50 (**B**), 100 (**C**), and 300 K (**D**). As expected, the data reflects an absence of temperature dependence for the diamagnetic control. These data points were used to correct for diamagnetism present in **HC**$^{\bullet 7+}$.

Finally, the iron contents of both the magnetic sample (**HC**$^{\bullet 7+}$) and the diamagnetic control (**CBPQT**•$4PF_6$) were determined by ICP-MS and were found to be very low with concentrations of 1.2 ppm and 0.8 ppm for **HC**$^{\bullet 7+}$ and **CBPQT**•$4PF_6$, respectively.

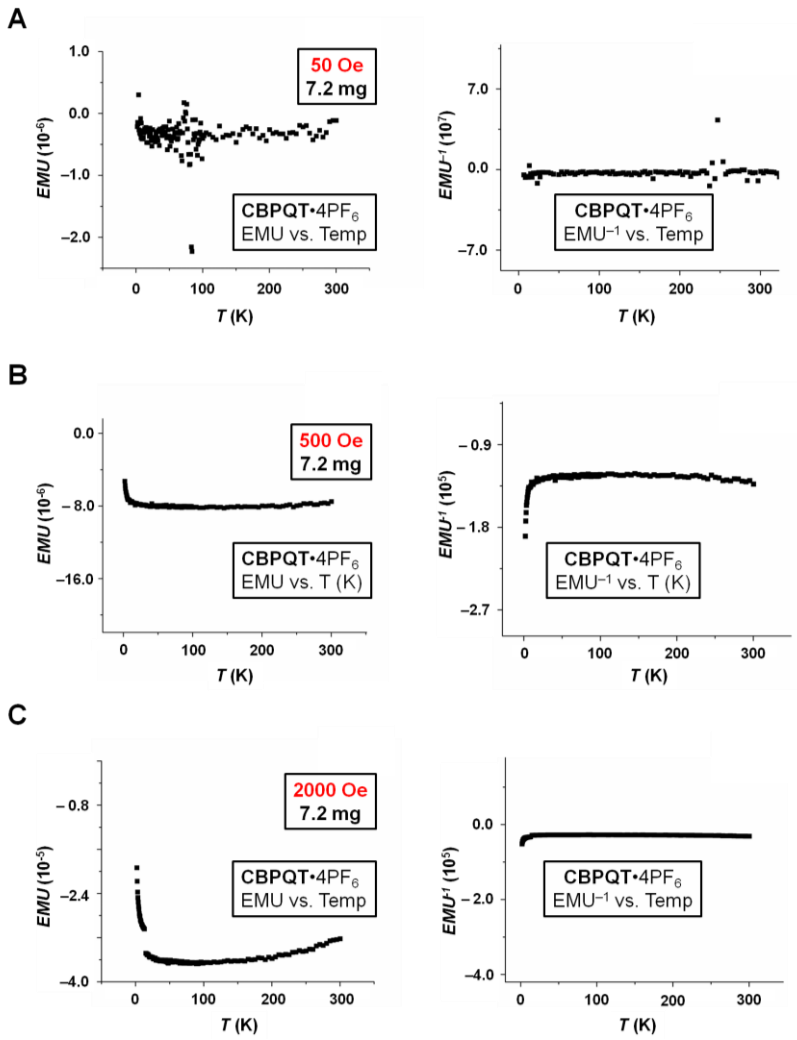

Fig. S16 Magnetization (*EMU*) versus temperature (K) and the corresponding reciprocal magnetization (EMU^{-1}) versus temperature (K) plots of **CBPQT**•$4PF_6$. This data shows the diamagnetic nature of the control compound is not greatly affected by the rise in temperature. These data points were used to correct for diamagnetism present in $\mathbf{HC}^{\bullet 7+}$.

e) High resolution mass spectrum (HRMS) of ***HC****•7PF$_6$(****HC****•6PF$_6$).* High-resolution mass spectrometry electrospray ionization (HRMS-ESI) was performed (fig. S17) on an MeCN solution of the homo[2]catenane directly after being purified and exposed to ambient O_2. The monoradical-heptacation **HC**•$7PF_6$, and the bisradical-hexacation **HC**•$6PF_6$ were observed in the mass spectrum, which displayed two sets of peaks for **HC**•$7PF_6$ – one set corresponding to the loss of one PF_6^- counterion, and the other corresponding to the loss of two PF_6^- counterions – while only one peak for **HC**•$6PF_6$ was observed, corresponding to the loss of two PF_6^- counterions. This data supports the notion that the oxidation to the 7^+ redox state is slow and

that an equilibrium exists between the $\mathbf{HC}^{2\bullet 6+}$ and $\mathbf{HC}^{\bullet 7+}$ in the starting state (bench-top) material.

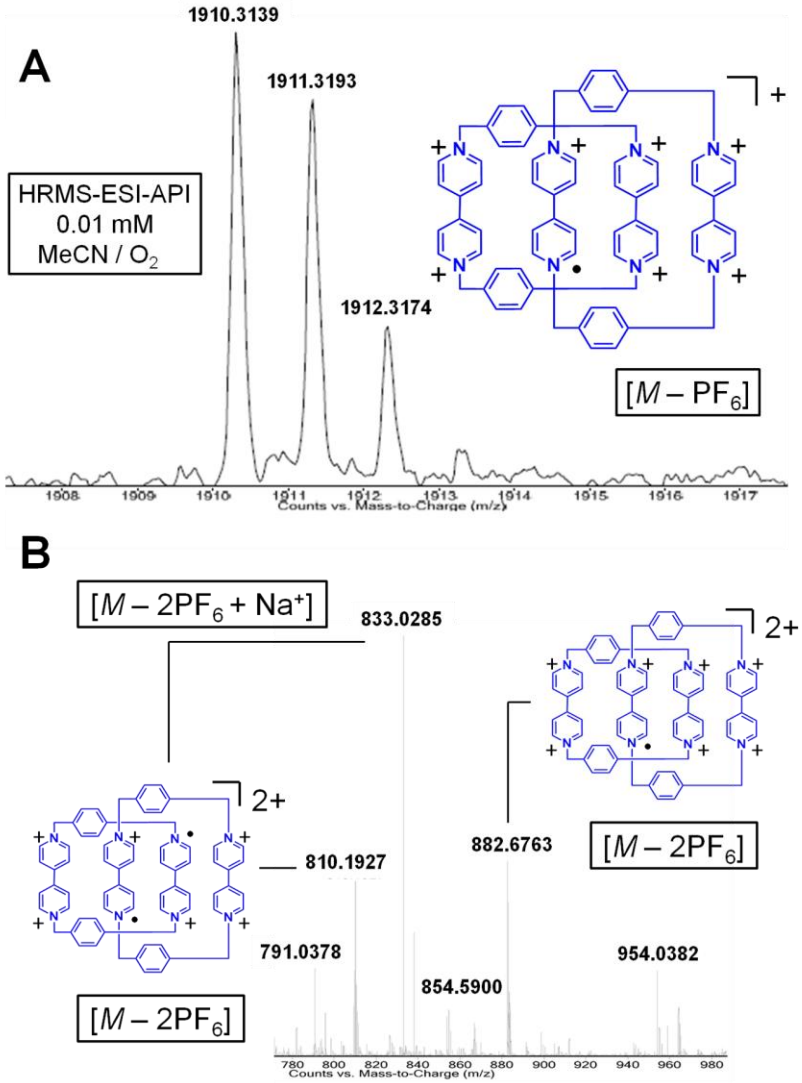

Fig. S17 HRMS-ESI-API analysis of **HC**•$7PF_6$ and **HC**•$6PF_6$. (**A**) For **HC**•$7PF_6$, Calcd for $C_{72}H_{64}F_{42}N_8P_7$: 1910.3116 $[M - PF_6]^+$, 882.6734 $[M - 2PF_6]^{2+}$; found: 1910.3139 $[M - PF_6]^+$, 882.6763 $[M - 2PF_6]^{2+}$. (**B**) For **HC**•$6PF_6$, Calcd for $C_{72}H_{64}F_{36}N_8P_6$: 810.1910 $[M - 2PF_6]^{2+}$, found 810.1927 $[M - 2PF_6]^{2+}$.

f) Cyclic Voltammetry (CV) / Michaelis' method. Cyclic voltammetry was performed (fig. S18) on a solution of the homo[2]catenane in DMF in order to supplement the electrochemical data obtained from square-wave differential pulse voltammetry (DPV). The redox potentials

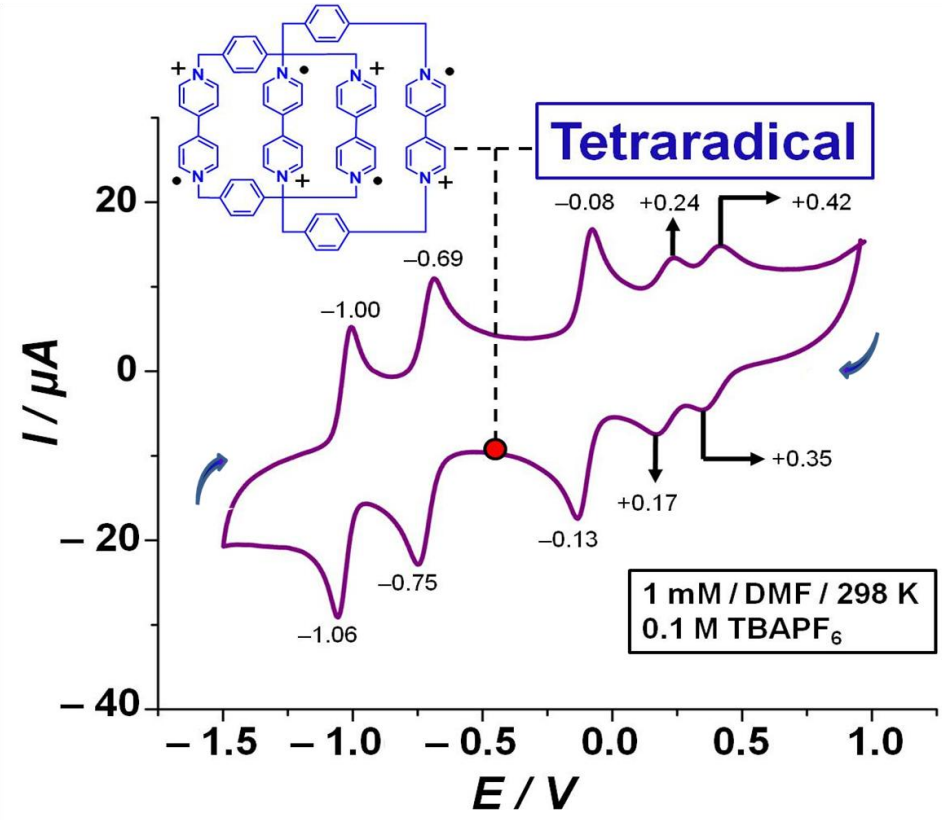

Fig. S18 Cyclic voltammogram of a 1 mM solution of the homo[2]catenane in DMF vs. a Ag/AgCl reference (0.1M $TBAPF_6$). The complete redox process is fully reversible. Note that, a total of six redox states are accessible electrochemically.

determined from CV match those measured from DPV. Each reduction wave is observed to have an oxidation wave of nearly identical peak current intensity, indicating the reversibility of each of these redox processes. The separation between cathodic and anodic peaks reveal that heterogeneous electron transfer is fast on the timescale of the experiment employing a scan rate of 200 mV s^{-1}.

Using Michaelis' method (*11*) for a one-electron reversible redox process, and the potentials from fig. S18 for the monoradical (+0.35 V) and bisradical (+0.17 V) states, the equilibrium constant, *K*, can be calculated (eq. S5) giving us an idea of the nature of the equilibrium between the 6^+ and 7^+ redox states. Using the Nernst equation we arrive at,

$$\log K = \frac{E_2 - E_1}{0.06} \qquad \text{(where } E \text{ is in V, and } T = 298 \text{ K)} \qquad \textit{Eqn. S5}$$

$$\log K = \frac{0.35 - 0.17}{0.06} = 3 \quad \text{and} \quad K = 1000$$

Although this value of K suggests the equilibrium favors the 7+ redox state by three orders of magnitude, this equilibrium constant seems a bit high because of the observation of the relative signal intensities in the EPR spectra (Fig. 2B) and a considerable broad band in the NIR of the starting state optical absorption spectrum of the homo[2]catenane (fig. S10A).

2) Bisbromomethyl(bis-p-benzylbipyridine) (DB•2PF$_6$)

*a) Analytical HPLC analysis of **DB**•2PF$_6$*

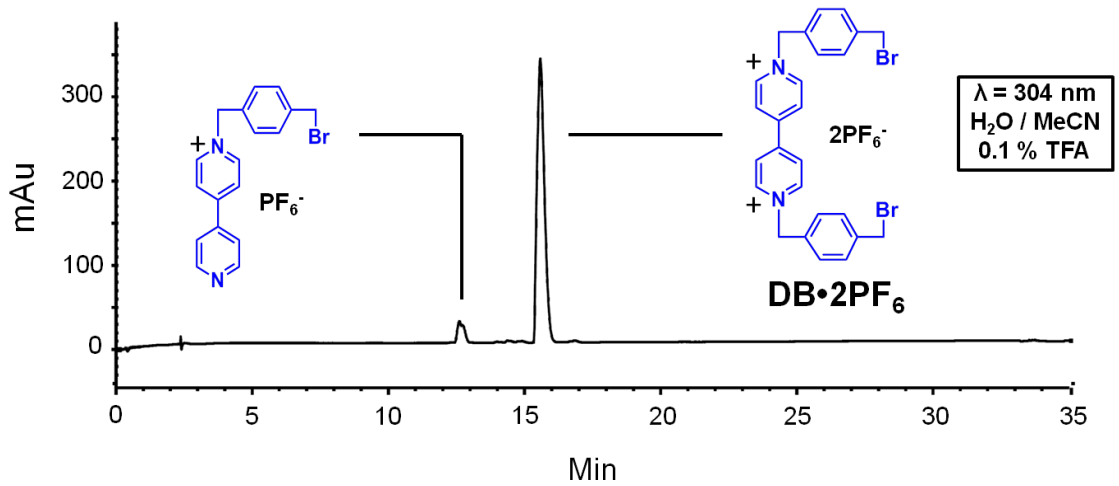

Fig. S19 Analytical RP-HPLC of the dibromo precursor **DB**•2PF$_6$.

b) ^{1}H NMR and ^{13}C NMR spectroscopic analysis

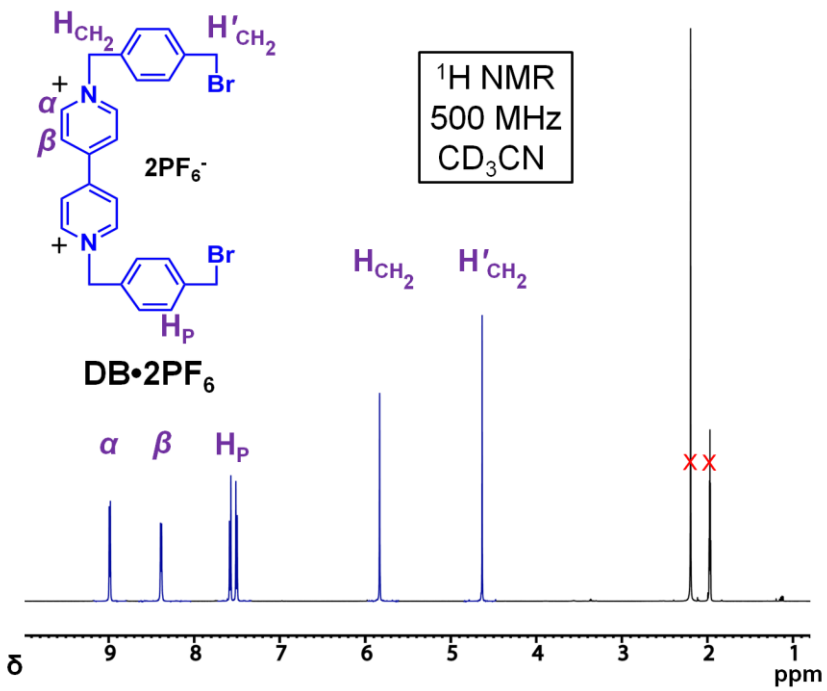

Fig. S20 ^{1}H NMR spectrum of **DB•**$2PF_6$**.** (500 MHz / CD_3CN / 298 K)

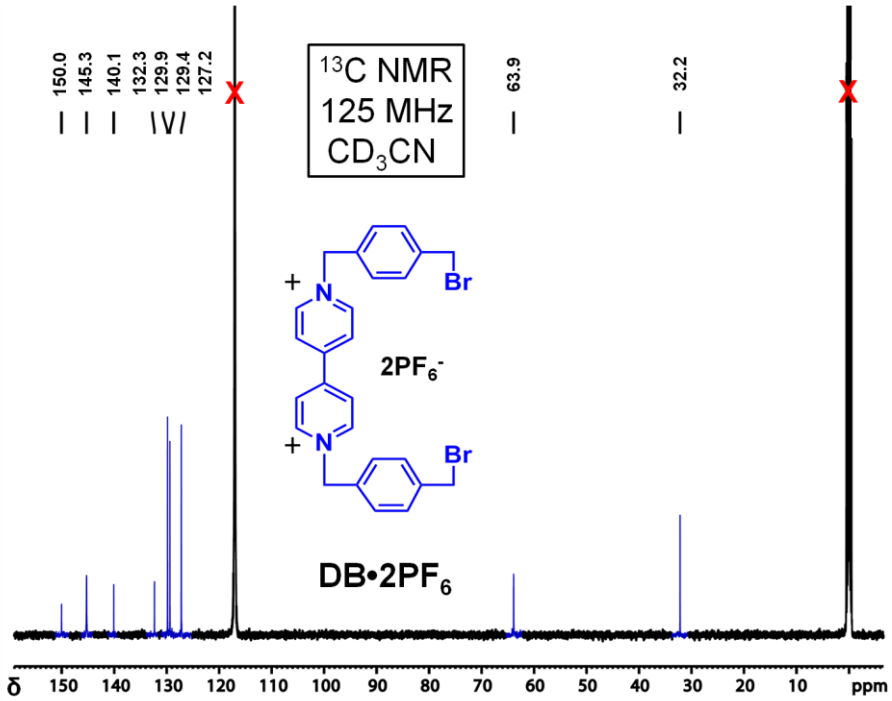

Fig. S21 ^{13}C NMR spectrum of **DB•**$2PF_6$**.** (125 MHz / CD_3CN / 298 K)

c) Low resolution mass spectrum (LRMS-ESI)

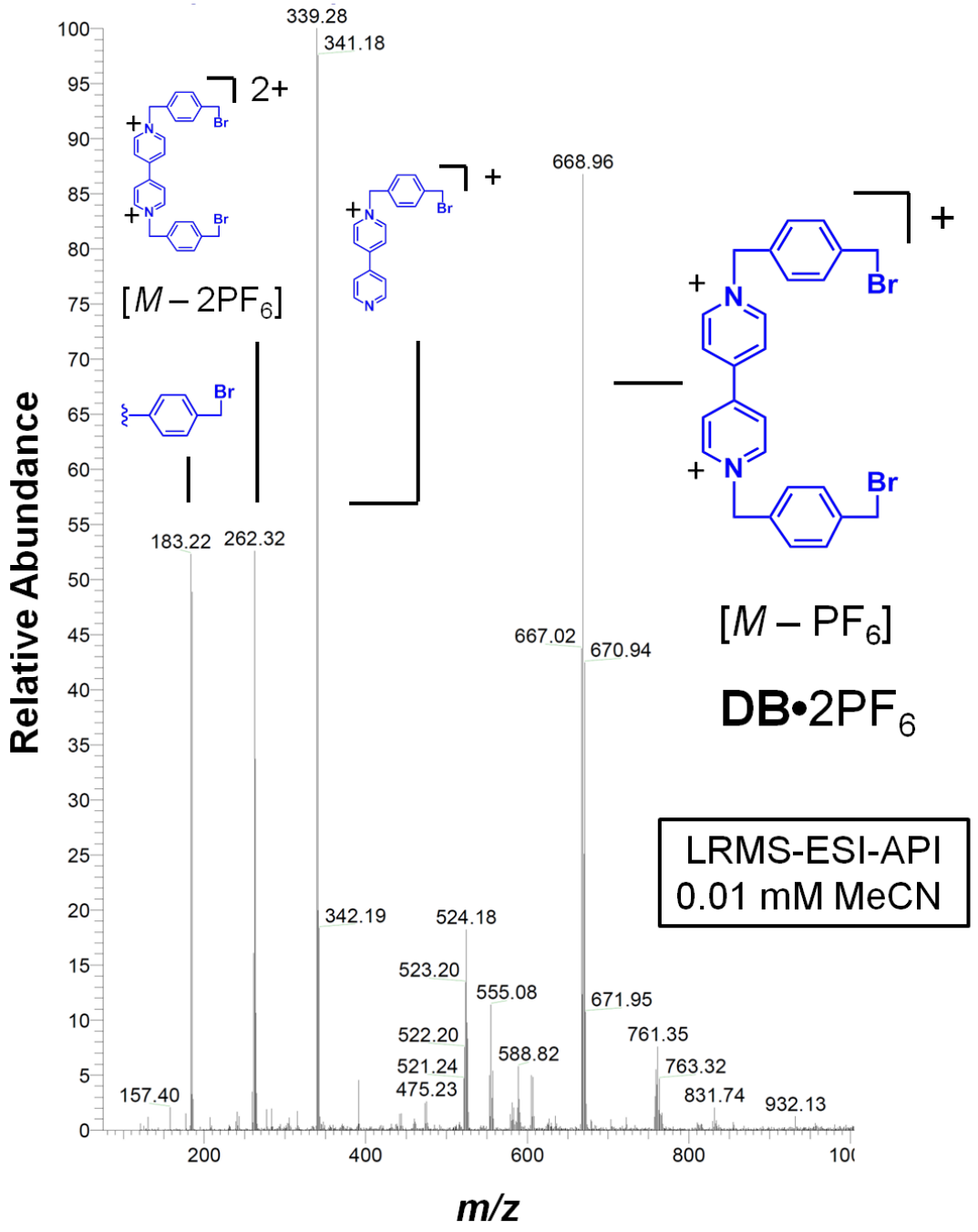

Fig. S22 Low-resolution mass spectrum (LRMS) for **DB**•$2PF_6$.

Section E. Computational Analysis

1) Methods

Calculations were performed using density functional theory (DFT) with the M06 functional, as implemented (*30*) in Jaguar 7.6.110. Geometry optimizations were performed (*41*) using the 6-31G* basis set. Electronic energies were obtained (*42*) using the 6-311++G** basis set. Solvent corrections were based on single point self-consistent Poisson-Boltzmann continuum solvation calculations for MeCN ($\varepsilon = 37.5$ and $R_0 = 2.179$ Å using (*43*) the PBF module in Jaguar.

2) Orbital Depictions of Additional Redox States

Fig. S23 shows the additional orbital depictions for some of the remaining redox states of the

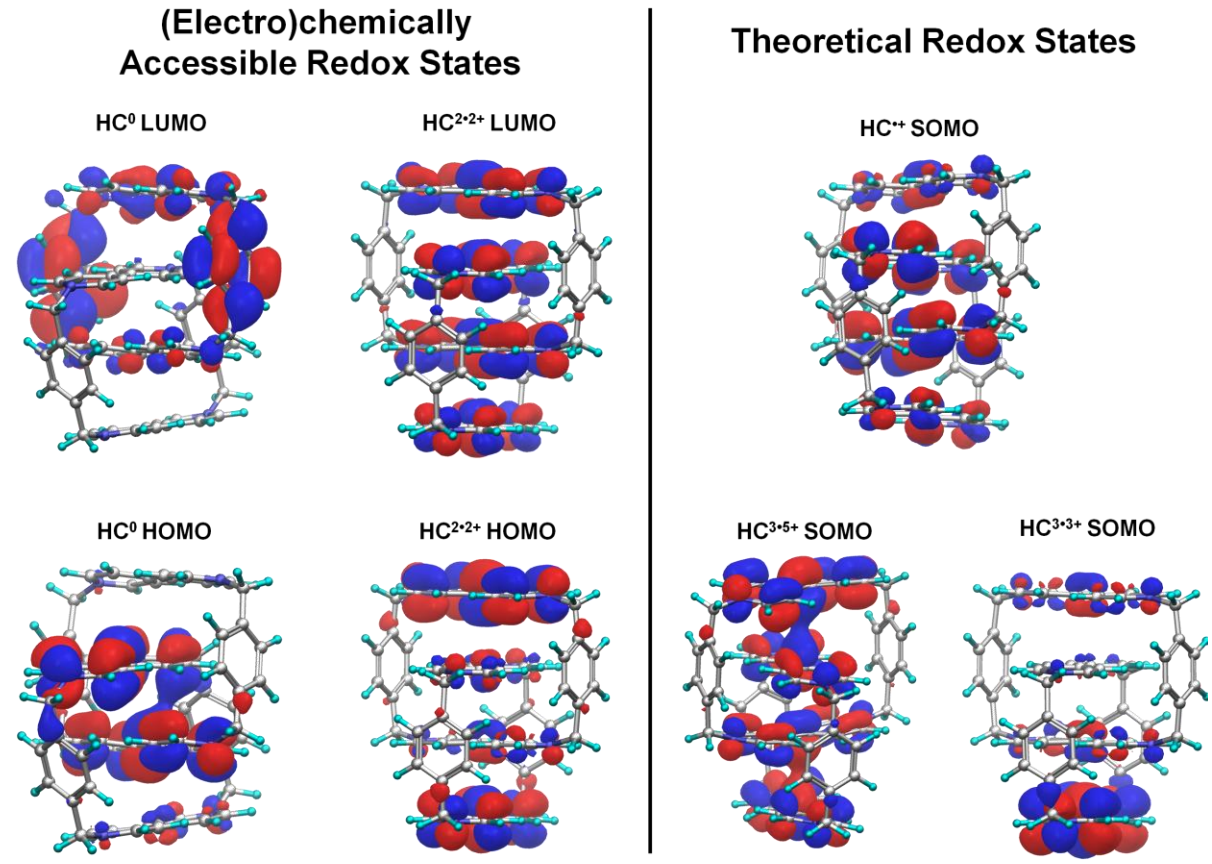

Fig. S23 DFT orbital depictions for the additional redox states. Additional orbital depictions for the experimentally observed redox states are shown on the left. The orbital depictions shown on the right have only been characterized by theory thus far. These results support the notion that electronic delocalization occurs over both inside $BIPY^{\bullet+}$ units, nearly equally in each case.

homo[2]catenane. For **HC**$^{2\bullet 2+}$ there are six electrons in the four MO's derived from the four SOVBO's resulting in three doubly occupied MO's. The HOMO is on BIPY units A and D so that BIPY's B and C each have two electrons. The LUMO is now fully antibonding, and a one-electron addition to the LUMO of **HC**$^{2\bullet 2+}$ leads to the formation of the SOMO of **HC**$^{\bullet +}$. Adding one electron to the SOMO of **HC**$^{\bullet +}$ generates the HOMO of **HC**^{0}. The LUMO now corresponds to some other part of the system. The trisradical (**HC**$^{3\bullet 5+}$ **SOMO**) is obtained by removing an electron from the tetraradical (**HC**$^{4(\bullet +)}$ **HOMO**, Fig. 4A), leading to similar orbital overlaps. The monoradical (**HC**$^{\bullet 7+}$ **SOMO**, Fig. 4A) is similar to the bisradical (**HC**$^{2\bullet 6+}$ **HOMO**, Fig. 4A) structure –which is corroborated through crystallographic analysis of the solid-state structures and EPR analysis of each redox state. The one-electron transition from **HC**$^{2\bullet 2+}$ to **HC**$^{3\bullet 3+}$ removes an electron from the **HC**$^{2\bullet 2+}$ **HOMO** to form the **HC**$^{3\bullet 3+}$ **SUMO**. Note, some slight asymmetry is probably due to slight distortions.

3) Calculated Binding Energies and Predicted Redox Potentials

The energies (internal energies comparable to enthalpies) for the process of formation of the homo[2]catenane are shown in table S1. The three columns on the left refer to the oxidation state under investigation. The first row corresponds to the reaction between **CBPQT**^{0} + **CBPQT**^{0} that makes the neutral **HC**^{0}. The last row corresponds to **CBPQT**$^{4+}$ + **CBPQT**$^{4+}$ that makes **HC**$^{8+}$. As seen in table S1, there is a big difference in the energy that leads to the formation of the **HC**$^{2\bullet 2+}$ if it is derived from the reaction of two radical cation **CBPQT**$^{\bullet +}$ species

Table S1. Calculated Binding Energies (kcal mol^{-1}) of the Homo[2]catenane

Charges			Energies (kcal mol^{-1})	
Product Ox. State	CBPQT 1 Ox. State	CBPQT 2 Ox. State	Gas Phase	CH_3CN
0	0	0	-40.4	-29.6
1	1	0	-54.3	-42
2	2	0	-117.5	-93
2	1	1	-17.7	-50.5
3	3	0	-115.7	-66
3	2	1	-26.6	-92
4	4	0	-155.6	-77
4	3	1	31.6	-58.3
4	2	2	20.9	-126.8
5	4	1	53.3	-50.2
5	3	2	140.8	-74
6	4	2	203.1	-54
6	3	3	301.3	-9.3
7	4	3	427.3	17
8	4	4	619	66.5

(–50.5 kcal mol^{-1}) or if it comes from a dication **CBPQT$^{2(\bullet+)}$** and the neutral **CBPQT^{0}** (–93.0 kcal mol^{-1}). This trend is reversed in the case of the formation of **HC$^{4(\bullet+)}$**, wherein it is more exothermic to form this product from two **CBPQT$^{2(\bullet+)}$** than from the tetracationic **CBPQT^{4+}** and the neutral **CBPQT^{0}**. These differences can be attributed to the electron pairing and formation of some degree of covalent bonds in the homo[2]catenane. In comparison with the proposed "as synthesized" product formed during the experiment, it is seen in Table 1 that the product is not formed unless the oxidation state and charge of the CBPQT is lower or equal to +2. The reaction for the **HC$^{4(\bullet+)}$** formed by combining two **CBPQT$^{2(\bullet+)}$** molecules turns out to be the most exothermic (–126.8 kcal mol^{-1}) of all because it involves pairing of both radical cations in each **CBPQT$^{2(\bullet+)}$** unit, which was corroborated the EPR data for **HC$^{4(\bullet+)}$**.

Using the computed energies (table S1), it was possible to predict (table S2) the redox potential for each oxidation state. The potentials listed in bold in Table S1 are the predicted reduction potentials for the (electro)chemically accessible states, while the non-bold reduction potentials are for the hypothetical redox states. The predicted values match the experimental redox potentials shown in fig. S18 quite well, even considering the CV data was collected in DMF, while the predictions were calculated for MeCN.

Table S2. Predicted redox potentials of the homo[2]catenane.

	Single Point Gas Phase 6-311G**++	LACVP**M06 SOLV MeCN					Predicted
Molecule (charge)	E_{SCF}	Vsolv	E	ΔE (kcal)	Abs Pot (V)	Redox Transition	Redox Potential (V, Ag/AgCl)
CBPQT(0)	-1609.177943	-17.0543	-1009791.66				
CBPQT(1)	-1609.008473	-43.0528	-1009711.32	80.35	1.74	CBPQT(0) to CBPQT(1)	
CBPQT(2)	-1608.680042	-126.2491	-1009588.42	122.90	2.66	CBPQT(1) to CBPQT(2)	
CBPQT(3)	-1608.368694	-267.2574	-1009534.05	177.26	3.84	CBPQT(2) to CBPQT(3)	
CBPQT(4)	-1607.90086	-461.7503	-1009434.98	99.08	2.15	CBPQT(3)to CBPQT(4)	
HC(0)	-3218.42021	-23.3109	-2019612.89				
HC(1)	-3218.272878	-47.8792	-2019545.01	67.88	1.47	HC(0) to HC(1)	-1.20
HC(2)	-3218.045187	-118.8512	-2019473.10	71.91	1.56	HC(1) to HC(2)	**-1.11**
HC(3)	-3217.73097	-234.6809	-2019391.75	81.34	1.76	HC(2) to HC(3)	-0.91
HC(4)	-3217.326841	-400.1937	-2019303.67	88.08	1.91	HC(3) to HC(4)	**-0.76**
HC(5)	-3216.824338	-608.3176	-2019196.47	107.20	2.32	HC(4) to HC(5)	-0.35
HC(6)	-3216.257169	-845.152	-2019077.40	119.07	2.58	HC(5)to HC(6)	**-0.09**
HC(7)	-3215.588657	-1139.313	-2018952.07	125.34	2.72	HC(6) to HC(7)	**+0.05**
HC(8)	-3214.815266	-1475.9905	-2018803.43	148.63	3.22	HC(7)to HC(8)	**+0.55**

Table S3. XYZ Coordinates Used in Calculating the Binding Energies

$HC^{0\bullet 0+}$	X	Y	Z
N1	0.0000000000	0.0000000000	0.0000000000
N2	0.0000000000	0.0000000000	7.1373530397
N3	6.8403349467	0.0000000000	-0.8365942318
N4	6.8523509777	0.2922105670	6.3097659819
C5	-0.1408115304	-1.1782430310	0.7113764330
H6	-0.2175912639	-2.0782610812	0.1021752593
C7	-0.2242052088	-1.2114105022	2.0583242762
H8	-0.3833096650	-2.1853530152	2.5186662580
C9	-0.1374164591	-0.0142982341	2.8768239336
C10	0.0296075521	1.1895909656	2.0825496381
H11	0.1386528699	2.1564073695	2.5659966651
C12	0.1128953330	1.1689146426	0.7399325006
H13	0.2672808052	2.0732246795	0.1540825139
C14	-0.1814818765	-0.0114598527	4.2555853518
C15	-0.2541928076	-1.2107616056	5.0738593098
H16	-0.4234277981	-2.1825889398	4.6121676074
C17	-0.1172464476	-1.1826900633	6.4151804205
H18	-0.1516386750	-2.0870704006	7.0231948593
C19	-0.0261534873	1.1813264503	6.3952649917
H20	-0.0048424166	2.0938883142	6.9899736987
C21	-0.1238160419	1.2002312556	5.0550683201
H22	-0.1869991326	2.1744066870	4.5772605074
C23	0.6917997795	0.0033766724	8.4194278840
H24	0.3123317170	0.8588490415	8.9989599915
H25	0.3984320870	-0.9089304093	8.9590201145
C26	2.1931652426	0.0851271229	8.2964102925
C27	2.9819580804	-1.0649763075	8.2895662967
H28	2.5095385159	-2.0400546615	8.4277000585
C29	4.3609402794	-0.9806607957	8.1266296844
H30	4.9655536261	-1.8902520666	8.1509737343
C31	4.9876599002	0.2537349291	7.9499681876
C32	4.1973321631	1.4031290125	7.9561695148
H33	4.6706703455	2.3788584731	7.8275522761
C34	2.8225509971	1.3208510367	8.1334095299
H35	2.2254103366	2.2336377677	8.1520082025
C36	6.4749560355	0.3432620566	7.7110508503
H37	6.9871641658	-0.4818997464	8.2299742237
H38	6.8713723686	1.2804602117	8.1276623542
C39	6.8892440666	1.4455310212	5.5350224824
H40	6.9237563584	2.3821982883	6.0935744040
C41	6.9177384080	1.4170336272	4.1871523576

H42	6.9752604288	2.3764523719	3.6768884044
C43	6.8456759017	0.1807623303	3.4333122546
C44	6.7367238875	-0.9894205523	4.2803522170
H45	6.6679067153	-1.9882380050	3.8518476212
C46	6.7341859219	-0.9107693051	5.6245776611
H47	6.6772146785	-1.8005620361	6.2511846397
C48	6.8660185454	0.1222182540	2.0543132553
C49	6.9823577703	1.2887258320	1.2000677846
H50	7.1134984093	2.2802242148	1.6302042700
C51	6.9331675650	1.2113050824	-0.1427424558
H52	7.0046005210	2.1000899057	-0.7731193660
C53	6.7476216383	-1.1464834124	-0.0414792345
H54	6.6970431854	-2.0828504383	-0.5980982562
C55	6.7676030572	-1.1155767190	1.3039852200
H56	6.7428993869	-2.0738118041	1.8220908103
C57	6.1601270633	-0.0178714352	-2.1260620439
H58	6.5100487957	0.8532753187	-2.6990359050
H59	6.4938413081	-0.9175203438	-2.6658173806
C60	4.6561101485	-0.0085814443	-2.0152665548
C61	3.9379322246	1.1867766790	-2.0160815800
H62	4.4680890136	2.1297991089	-2.1653359129
C63	2.5584405716	1.1912909344	-1.8381387712
H64	2.0150932998	2.1378980978	-1.8508875994
C65	1.8595166009	-0.0004229882	-1.6491720891
C66	2.5754833428	-1.1977187812	-1.6609309521
H67	2.0413314957	-2.1419236432	-1.5354866903
C68	3.9520232801	-1.2020615290	-1.8410463411
H69	4.4919080319	-2.1498974384	-1.8577092790
C70	0.3705987285	-0.0034309584	-1.4062361667
H71	-0.0882296286	-0.8913590614	-1.8647551232
H72	-0.0920019877	0.8762080466	-1.8784849659
N73	8.5471176375	-5.0357540559	3.8532700871
N74	10.8848547874	1.6614972037	2.9691754947
N75	2.9535317708	-1.2092039547	3.3954350238
N76	5.1416217810	5.4925549558	2.2780838339
C77	8.7297306459	-4.4702391106	2.5861225216
H78	8.4701839670	-5.1285368426	1.7568413433
C79	9.2261462102	-3.2347956370	2.3910160586
H80	9.3700728864	-2.9135604864	1.3614561651
C81	9.5790200226	-2.3522232207	3.4899854575
C82	9.4306059859	-2.9917508706	4.7857027665
H83	9.7485251039	-2.4752681187	5.6892463219
C84	8.9247097286	-4.2292413485	4.9316633449
H85	8.8182917866	-4.7018600459	5.9085834803
C86	9.9886810086	-1.0448224282	3.3235407912
C87	10.1198552263	-0.4037811452	2.0290288328

H88	9.8458328762	-0.9337973377	1.1195325348
C89	10.5299389386	0.8708102727	1.8891694092
H90	10.5971175108	1.3553627628	0.9163446712
C91	10.7101288215	1.1191480517	4.2286543051
H92	10.9362149832	1.7897653086	5.0561830109
C93	10.3022243628	-0.1516721707	4.4237490052
H94	10.1947875970	-0.4832175643	5.4532674933
C95	11.1537287612	3.0755593699	2.7771826971
H96	11.7422905415	3.4184074288	3.6402696073
H97	11.7993891367	3.1791332029	1.8919356389
C98	9.9207649340	3.9285231354	2.6139157577
C99	9.4579411706	4.2892782594	1.3497160958
H100	10.0036698934	3.9588046214	0.4639780103
C101	8.3172064816	5.0724909386	1.2062793639
H102	7.9693107560	5.3479134352	0.2087836908
C103	7.6159335674	5.5255716366	2.3226536181
C104	8.0764632197	5.1549130371	3.5890891557
H105	7.5394573885	5.4961116804	4.4748046615
C106	9.2092631843	4.3661901663	3.7315397629
H107	9.5551264051	4.0904473596	4.7298295544
C108	6.3434950061	6.3176074857	2.1738165598
H109	6.3188073057	6.8266898670	1.1985390916
H110	6.2776882952	7.0956476266	2.9491784567
C111	4.8219524656	5.0076016317	3.5539730261
H112	4.9541725248	5.7347664851	4.3565155946
C113	4.3415321929	3.7716732793	3.7793678113
H114	4.0756176175	3.5200737304	4.8044838791
C115	4.1461277431	2.8042486093	2.7122508743
C116	4.4078152681	3.3627795502	1.3976054395
H117	4.1861126290	2.7752460039	0.5075007225
C118	4.8920593829	4.6041228526	1.2191582528
H119	5.0796237280	5.0212527070	0.2285498301
C120	3.7659404147	1.4935063818	2.9271195788
C121	3.4757886103	0.9601489566	4.2410246224
H122	3.5506717165	1.5862646259	5.1269251013
C123	3.1010112354	-0.3192292488	4.4370697897
H124	2.8707575224	-0.7094306065	5.4290785912
C125	3.2591891480	-0.7632510283	2.1246281253
H126	3.1759338615	-1.5063114774	1.3320369230
C127	3.6318702025	0.5084266791	1.8726010114
H128	3.8660556418	0.7578020961	0.8387102266
C129	2.5989485943	-2.5951072162	3.6340931943
H130	2.0071566773	-2.6210847508	4.5604153353
H131	1.9296102392	-2.9142964624	2.8188364899
C132	3.7898103455	-3.5093771971	3.7456770873
C133	4.4453724704	-3.6637180591	4.9679888475

H134	4.0640404581	-3.1358732907	5.8458892900
C135	5.5743040016	-4.4655874984	5.0727245299
H136	6.0744821880	-4.5760040640	6.0374188606
C137	6.0821686677	-5.1336755634	3.9560309061
C138	5.4200615861	-4.9840540560	2.7381031749
H139	5.7975428084	-5.5062920250	1.8571257843
C140	4.2873343263	-4.1854050475	2.6343716671
H141	3.7786347633	-4.0853897715	1.6735714019
C142	7.3786094080	-5.8965753853	4.0326621259
H143	7.4127494657	-6.6753256731	3.2561446936
H144	7.4851111405	-6.3988753134	5.0052985729

$HC^{1\bullet 1+}$	**X**	**Y**	**Z**
N1	0.0000000000	0.0000000000	0.0000000000
N2	0.0000000000	0.0000000000	7.1516419862
N3	6.6657976420	0.0000000000	-0.0013052157
N4	6.6724715907	0.1676237415	7.1247653821
C5	-0.0428508781	-1.1820356656	0.7250172793
H6	-0.1275531663	-2.0871259355	0.1253284613
C7	-0.0360753165	-1.2125800285	2.0740354333
H8	-0.1202145077	-2.1890026290	2.5447656821
C9	0.0409570865	-0.0124262914	2.8832633061
C10	0.1310138861	1.1916461732	2.0817951840
H11	0.2197173832	2.1664418553	2.5556753868
C12	0.1289148619	1.1707686198	0.7343524277
H13	0.2127091622	2.0804470707	0.1414110343
C14	0.0306248420	-0.0128427224	4.2679470713
C15	-0.0231808474	-1.2139197140	5.0788934403
H16	-0.0708243225	-2.1938152721	4.6093343430
C17	-0.0090890171	-1.1831110890	6.4274950643
H18	-0.0370898148	-2.0901283842	7.0306618313
C19	0.0543002214	1.1757929932	6.4157975470
H20	0.0408082343	2.0898989878	7.0072078709
C21	0.0625494222	1.1956401862	5.0678230993
H22	0.0587641943	2.1725167090	4.5912647498
C23	0.4414854042	0.0062931401	8.5410374496
H24	-0.0185751166	0.8747493802	9.0342310354
H25	0.0375533664	-0.8923200387	9.0273944937
C26	1.9433726358	0.0562404274	8.6699533740
C27	2.6954225324	-1.0991514704	8.8749394813
H28	2.1839136744	-2.0502196419	9.0363723632
C29	4.0865217345	-1.0523075422	8.8783842097
H30	4.6600654285	-1.9667609901	9.0454752682
C31	4.7592634350	0.1504140568	8.6705487147

C32	4.0061274911	1.3139016081	8.5036483396
H33	4.5146120705	2.2707195183	8.3739264073
C34	2.6200499291	1.2679067711	8.5075940044
H35	2.0504168148	2.1896441998	8.3859811742
C36	6.2580414740	0.1950203735	8.5275028477
H37	6.7272880586	-0.6601905312	9.0335049009
H38	6.6727955691	1.1072412079	8.9774949084
C39	6.7062268046	1.3311378914	6.3806360273
H40	6.7422697841	2.2513473902	6.9609443939
C41	6.7329573912	1.3281798513	5.0274194241
H42	6.8031004719	2.2939631372	4.5311467025
C43	6.6938257266	0.1074286395	4.2598313641
C44	6.6544023815	-1.0776950175	5.0763433193
H45	6.6478734461	-2.0718058765	4.6318535199
C46	6.6247178617	-1.0212058522	6.4275680163
H47	6.5862182896	-1.9219199682	7.0393964821
C48	6.6955495195	0.0768146930	2.8603544949
C49	6.7020713314	1.2583570145	2.0379209375
H50	6.7310268364	2.2546561830	2.4769725365
C51	6.6593189069	1.1943770811	0.6871826323
H52	6.6445344338	2.0925805804	0.0704644289
C53	6.6770994097	-1.1590804325	0.7487392787
H54	6.6940888241	-2.0835543529	0.1743383052
C55	6.7005951796	-1.1494140980	2.1012102274
H56	6.7549701580	-2.1139102339	2.6012565277
C57	6.2435370361	-0.0372468342	-1.4007005549
H58	6.6833511017	0.8326475074	-1.9073963381
H59	6.6827072967	-0.9353205065	-1.8552719160
C60	4.7436706703	-0.0394554932	-1.5362087769
C61	4.0355616103	1.1439540395	-1.7368470717
H62	4.5824145225	2.0763504356	-1.8955766251
C63	2.6445451971	1.1482984176	-1.7357624715
H64	2.1044916115	2.0837595044	-1.8937275192
C65	1.9272100587	-0.0299583190	-1.5333124106
C66	2.6382301172	-1.2211717011	-1.3698594566
H67	2.0947720635	-2.1584224426	-1.2425913417
C68	4.0259372169	-1.2259115942	-1.3718658617
H69	4.5626782253	-2.1677577882	-1.2477219757
C70	0.4258898223	-0.0164457822	-1.3943018558
H71	-0.0200343271	-0.9024002994	-1.8672569165
H72	-0.0023330879	0.8654863508	-1.8912019516
N73	9.8994630759	-3.6160693984	4.6440662978
N74	10.2107177036	3.1400561244	2.3290379936
N75	3.2756903575	-2.9086116458	4.4826988089
N76	3.5438408000	3.8829964686	2.3527077006
C77	9.9294431432	-3.3089603949	3.2908486283

H78	9.9484776664	-4.1702485323	2.6244651041
C79	9.9881336742	-2.0431845949	2.8284685017
H80	10.0606071454	-1.9150677258	1.7514693579
C81	9.9981381095	-0.8910867961	3.7066994228
C82	9.9584649772	-1.2585168752	5.1075866127
H83	9.9720796953	-0.4918826971	5.8798187178
C84	9.8901280198	-2.5397829636	5.5212762061
H85	9.8467456319	-2.8073277943	6.5763178704
C86	10.0511784601	0.4192445201	3.2562115528
C87	10.0745529432	0.7911822702	1.8562079800
H88	10.0430519963	0.0279565825	1.0816425627
C89	10.1265495440	2.0757700955	1.4466795917
H90	10.1298815425	2.3494884638	0.3923717129
C91	10.1708199819	2.8331565522	3.6794251947
H92	10.2389778453	3.6881981616	4.3497544577
C93	10.1032972749	1.5666417001	4.1380006253
H94	10.1168075709	1.4335506342	5.2164888470
C95	9.8986467305	4.4924631564	1.8834717632
H96	10.4155819613	5.1924580498	2.5551732273
H97	10.3332460583	4.6259889183	0.8832266097
C98	8.4168015953	4.7718460158	1.8628662841
C99	7.6723796945	4.6410571091	0.6911248612
H100	8.1832144915	4.4068633653	-0.2449952830
C101	6.2909729763	4.8076097218	0.7026834308
H102	5.7239893627	4.7036578708	-0.2253149605
C103	5.6191088540	5.1095350893	1.8868225679
C104	6.3678184463	5.2665055448	3.0551024858
H105	5.8637391974	5.5284882548	3.9865326848
C106	7.7455356617	5.1021846996	3.0426784442
H107	8.3126217488	5.2408230311	3.9640548857
C108	4.1148716205	5.1634123370	1.9372620331
H109	3.6961113588	5.4161019878	0.9532501089
H110	3.7687980421	5.9280726767	2.6461124293
C111	3.5148451234	3.5503617945	3.6957618086
H112	3.5230253416	4.3970337417	4.3802726227
C113	3.4389021494	2.2718486264	4.1290127174
H114	3.3671580475	2.1137073174	5.2028325742
C115	3.4207452788	1.1518310814	3.2193271413
C116	3.4388757903	1.5427517130	1.8326658748
H117	3.3820541731	0.8007351515	1.0384273354
C118	3.5154382382	2.8361583531	1.4479117949
H119	3.5363353134	3.1259601123	0.3977749277
C120	3.3765387634	-0.1801108523	3.6398087638
C121	3.3644414271	-0.5767549808	5.0249453254
H122	3.3722692575	0.1601203189	5.8279909310
C123	3.3357690073	-1.8781058629	5.3951323152

H124	3.3332443841	-2.1778483625	6.4428357062
C125	3.2888087952	-2.5720225484	3.1440144603
H126	3.2340733487	-3.4114211668	2.4529270030
C127	3.3267078749	-1.2892073197	2.7185537070
H128	3.2875948311	-1.1232809245	1.6449537868
C129	3.5511448565	-4.2802672630	4.9042247875
H130	3.0667880604	-4.4350992069	5.8782646661
H131	3.0607272279	-4.9533805678	4.1873228400
C132	5.0279458627	-4.5665278926	4.9867546394
C133	5.7229341114	-4.4363411383	6.1881161219
H134	5.1727215793	-4.2112429102	7.1049307322
C135	7.1054325139	-4.5872428904	6.2296620421
H136	7.6347772385	-4.4801667946	7.1786494747
C137	7.8280317904	-4.8721826184	5.0715964589
C138	7.1256012391	-5.0421524046	3.8758668346
H139	7.6683030452	-5.2993267158	2.9654576731
C140	5.7464395554	-4.8912632554	3.8342028406
H141	5.2163503914	-5.0324387746	2.8908963510
C142	9.3354999289	-4.8916395291	5.0749021572
H143	9.7200146766	-5.6702315645	4.4012578618
H144	9.7224255732	-5.1111701337	6.0797257531

$HC^{2\bullet 2+}$	**X**	**Y**	**Z**
N1	0.0000000000	0.0000000000	0.0000000000
N2	0.0000000000	0.0000000000	7.1273814828
N3	6.5396741744	0.0000000000	0.0172001823
N4	6.5348982567	0.0372461496	7.1323997578
C5	0.0148788624	-1.1772321582	0.7191131278
H6	-0.0260539472	-2.0868695816	0.1234912612
C7	0.0281597230	-1.2024241474	2.0713237194
H8	-0.0104064382	-2.1792454771	2.5448416100
C9	0.0428334544	0.0019916836	2.8641645199
C10	0.0200815920	1.2037465618	2.0697883406
H11	-0.0054731671	2.1825571470	2.5422688553
C12	0.0185476884	1.1773063385	0.7166026953
H13	0.0048791734	2.0866528060	0.1182018095
C14	0.0440867988	0.0019031291	4.2630611480
C15	0.0480352121	-1.2007989191	5.0562260132
H16	0.0474028044	-2.1794662074	4.5826026700
C17	0.0435491118	-1.1759867393	6.4092176063
H18	0.0484439693	-2.0858332786	7.0067775048
C19	-0.0040059867	1.1783849419	6.4097345459
H20	-0.0595192995	2.0864393975	7.0067754581
C21	0.0082352994	1.2051560074	5.0572308679

H22	-0.0460996364	2.1817355818	4.5844663722
C23	0.3624773617	0.0060317595	8.5464660377
H24	-0.1013258409	0.8879319801	9.0073239603
H25	-0.0856555098	-0.8795923160	9.0151921105
C26	1.8592565803	0.0201010310	8.7146118020
C27	2.5784692123	-1.1647181413	8.8717164981
H28	2.0421697367	-2.1067154713	8.9989047020
C29	3.9695110941	-1.1550072458	8.8745203845
H30	4.5188018009	-2.0901891584	9.0033079006
C31	4.6719905075	0.0391166548	8.7185131596
C32	3.9521266346	1.2306059506	8.6092325343
H33	4.4848760265	2.1796827012	8.5339358837
C34	2.5647721814	1.2212118491	8.6077288814
H35	2.0193670317	2.1627056978	8.5316072783
C36	6.1672250640	0.0445669158	8.5550396738
H37	6.6279568919	-0.8335499851	9.0255125952
H38	6.6201016582	0.9345405919	9.0096998567
C39	6.5378191212	1.2108375656	6.4134421575
H40	6.5532335457	2.1223295194	7.0071926093
C41	6.5511183146	1.2296789879	5.0579964347
H42	6.5912025090	2.2043237311	4.5770710254
C43	6.5481389900	0.0197073736	4.2800219153
C44	6.5473841827	-1.1764461494	5.0702946677
H45	6.5660074390	-2.1643751086	4.6110837191
C46	6.5234261957	-1.1395811585	6.4273643649
H47	6.5137668379	-2.0505062804	7.0248595988
C48	6.5532928441	0.0153640853	2.8699774151
C49	6.5327460893	1.2129119905	2.0811084927
H50	6.5332371096	2.1995240695	2.5414614126
C51	6.5034139850	1.1762042852	0.7234511493
H52	6.4726370377	2.0864311064	0.1250541969
C53	6.5881790396	-1.1729437619	0.7346851574
H54	6.6353365408	-2.0821656021	0.1388772108
C55	6.6040614169	-1.1927429336	2.0906780620
H56	6.6850153728	-2.1651244878	2.5712971584
C57	6.1725236664	-0.0143647401	-1.4060937447
H58	6.6283267199	0.8653722421	-1.8790830649
H59	6.6317074439	-0.9033706964	-1.8576222116
C60	4.6769851925	-0.0172995883	-1.5731667496
C61	3.9684990419	1.1728038692	-1.7371829377
H62	4.5132925580	2.1105580661	-1.8682635781
C63	2.5772411132	1.1755103756	-1.7398350463
H64	2.0367759314	2.1147337264	-1.8714918758
C65	1.8631953950	-0.0122501641	-1.5821986305
C66	2.5744580757	-1.2095799612	-1.4699931609
H67	2.0337579586	-2.1536991071	-1.3945718083

C68	3.9619719727	-1.2121217455	-1.4640365681
H69	4.4992568791	-2.1582948048	-1.3828174567
C70	0.3657786271	-0.0043826234	-1.4181995968
H71	-0.0933815905	-0.8881107711	-1.8802493831
H72	-0.0850060204	0.8794466136	-1.8877641055
N73	9.9202368835	-3.3590766952	4.8857475414
N74	9.8114507663	3.4055882069	2.6508970099
N75	3.3741371397	-3.3435832222	4.6172498964
N76	3.2820597405	3.4256650379	2.4675778396
C77	9.9590410462	-3.0440938959	3.5424533338
H78	10.0644262143	-3.8921819465	2.8686533412
C79	9.9218659729	-1.7688132453	3.0938848362
H80	10.0105326219	-1.6223247886	2.0209935818
C81	9.8236137912	-0.6407708686	3.9872496991
C82	9.8024834699	-1.0178779785	5.3776642082
H83	9.7703920733	-0.2618229518	6.1586527188
C84	9.8296597388	-2.3109695123	5.7765509770
H85	9.8086247260	-2.5951239675	6.8273574980
C86	9.7880679337	0.6869227839	3.5488049560
C87	9.8260234483	1.0630693190	2.1578064927
H88	9.8667330334	0.3063285036	1.3773350584
C89	9.8203912721	2.3555388470	1.7572578715
H90	9.8476855341	2.6380718933	0.7062384664
C91	9.7585909551	3.0932124686	3.9938688122
H92	9.7653395660	3.9459873245	4.6696300388
C93	9.7477813408	1.8171861974	4.4449439812
H94	9.7555050334	1.6748298708	5.5215628249
C95	9.4648551346	4.7532683934	2.1951511811
H96	9.9073365085	5.4704776202	2.8988944481
H97	9.9451483937	4.9151962252	1.2213889989
C98	7.9703847574	4.9200327575	2.1071302263
C99	7.2875305801	4.6955858007	0.9112406893
H100	7.8523906802	4.5160562776	-0.0055753145
C101	5.8967732995	4.7046034996	0.8763079925
H102	5.3765520351	4.5328673780	-0.0688878203
C103	5.1579919360	4.9355682010	2.0364972990
C104	5.8420566573	5.2084320449	3.2229008244
H105	5.2815101935	5.4386019521	4.1300699891
C106	7.2290560116	5.2021419764	3.2573331005
H107	7.7462730186	5.4292607384	4.1904098955
C108	3.6613451212	4.7826729658	2.0476569931
H109	3.2296994660	4.9588047841	1.0538429485
H110	3.1878793584	5.4900549931	2.7407285895
C111	3.2412635627	3.1032892634	3.8051678975
H112	3.1955790967	3.9498403488	4.4870851306
C113	3.2334467047	1.8194644757	4.2412288190

H114	3.1608321898	1.6603574808	5.3140843898
C115	3.2835353228	0.7099354111	3.3267455777
C116	3.3010757552	1.0893265822	1.9441251569
H117	3.3056883877	0.3495830568	1.1460962191
C118	3.3224610891	2.3934647783	1.5642233470
H119	3.3524714896	2.6845633477	0.5147313111
C120	3.3047653524	-0.6317150003	3.7553673642
C121	3.3184890302	-1.0081352795	5.1391017334
H122	3.2949173997	-0.2661688660	5.9345690033
C123	3.3736887731	-2.3104572741	5.5204422208
H124	3.4008965462	-2.6000120691	6.5703968709
C125	3.3445164669	-3.0248187248	3.2791160635
H126	3.3343212344	-3.8730381506	2.5978493562
C127	3.3033559907	-1.7420591851	2.8402748914
H128	3.2441569348	-1.5853815995	1.7652109249
C129	3.7405512004	-4.6988551114	5.0532076119
H130	3.2500518584	-4.8854548123	6.0173456681
H131	3.3146898788	-5.4049946273	4.3288591576
C132	5.2341041147	-4.8512100249	5.1595770253
C133	5.8920007099	-4.6858974120	6.3774747645
H134	5.3090526351	-4.5524088822	7.2913023110
C135	7.2823598394	-4.6934505716	6.4395947778
H136	7.7839343784	-4.5645436299	7.4004708414
C137	8.0446761473	-4.8698399436	5.2853462522
C138	7.3824354332	-5.0864496244	4.0734889090
H139	7.9610672204	-5.2723058548	3.1680096762
C140	5.9971492510	-5.0760950530	4.0114386777
H141	5.4992957822	-5.2547611245	3.0570903383
C142	9.5425665022	-4.7103295451	5.3061483164
H143	10.0328782922	-5.4213371443	4.6283377310
H144	9.9515328105	-4.8817608554	6.3102715030

$HC^{3\bullet 3+}$	**X**	**Y**	**Z**
N1	0.0000000000	0.0000000000	0.0000000000
N2	0.0000000000	0.0000000000	7.1057257240
N3	6.5018869577	0.0000000000	-0.0490154927
N4	6.4837095221	0.2339439545	7.0792356684
C5	-0.0154945751	-1.1736572774	0.7059987912
H6	-0.0639079712	-2.0815788264	0.1094936325
C7	-0.0113661894	-1.1992836172	2.0648883309
H8	-0.0760315998	-2.1737593792	2.5388347145
C9	0.0156359240	0.0036517305	2.8418767531
C10	-0.0000933612	1.2012553199	2.0630754672
H11	-0.0218333724	2.1794100904	2.5358071093

C12	0.0117155182	1.1736036519	0.7020961847
H13	0.0085402623	2.0817392036	0.1029277665
C14	0.0143233111	0.0047975928	4.2632090371
C15	0.0546999119	-1.1940549100	5.0391109662
H16	0.0792519483	-2.1708686487	4.5644109570
C17	0.0668419516	-1.1691919540	6.4002846482
H18	0.1088868804	-2.0782758809	6.9968587913
C19	-0.0723368574	1.1739474820	6.4020022502
H20	-0.1644870295	2.0769523257	7.0007979932
C21	-0.0698305016	1.2031917633	5.0431952575
H22	-0.1789310378	2.1748768373	4.5712650582
C23	0.3327655455	0.0178090094	8.5430539983
H24	-0.1754221730	0.8799716484	8.9916604906
H25	-0.0899823500	-0.8853417408	8.9992396343
C26	1.8275129374	0.0905025452	8.7113114355
C27	2.5885405958	-1.0614852803	8.9076718712
H28	2.0888951747	-2.0163460214	9.0806127065
C29	3.9792719379	-0.9998350129	8.8987382864
H30	4.5623249690	-1.9078412391	9.0661747621
C31	4.6359368729	0.2120834312	8.6868936071
C32	3.8721307243	1.3731311512	8.5477425668
H33	4.3691979687	2.3383429718	8.4417194555
C34	2.4863041255	1.3136207867	8.5617520788
H35	1.9079324648	2.2336283509	8.4689411598
C36	6.1292646486	0.2690464148	8.5058656521
H37	6.6258826145	-0.5774154907	8.9976764984
H38	6.5535324313	1.1868503103	8.9323508481
C39	6.4913213981	1.3891304908	6.3271815292
H40	6.5117784498	2.3155656214	6.8976394704
C41	6.5055167537	1.3734323822	4.9716378589
H42	6.5500796036	2.3365396960	4.4666678126
C43	6.4959138578	0.1437869952	4.2163861967
C44	6.4923590884	-1.0325778451	5.0448398313
H45	6.5070705656	-2.0328103153	4.6123756386
C46	6.4658424374	-0.9602978040	6.3993705498
H47	6.4528357767	-1.8558199679	7.0202035441
C48	6.5049507961	0.0990519680	2.8126701979
C49	6.4830380938	1.2738687234	1.9812635924
H50	6.4789211626	2.2754844014	2.4107248021
C51	6.4626012945	1.1967083075	0.6268937609
H52	6.4353444607	2.0898153201	0.0028161103
C53	6.5339037400	-1.1521128475	0.7064350724
H54	6.5734274319	-2.0792572052	0.1379457878
C55	6.5459603795	-1.1329409268	2.0618062177
H56	6.6128053748	-2.0938827803	2.5701539194
C57	6.1252899950	-0.0510768745	-1.4697754060

H58	6.5852070044	0.8100740028	-1.9715108763
H59	6.5721584559	-0.9554961050	-1.9017828805
C60	4.6280797742	-0.0452656348	-1.6260647826
C61	3.9259440275	1.1495099858	-1.7868458177
H62	4.4749538207	2.0825514245	-1.9303303331
C63	2.5345180725	1.1614276249	-1.7810802367
H64	1.9992182717	2.1027905876	-1.9181484298
C65	1.8166905521	-0.0239251656	-1.6200513791
C66	2.5197518577	-1.2265323572	-1.5173463137
H67	1.9751502118	-2.1693266545	-1.4514933478
C68	3.9076680400	-1.2366109178	-1.5183784947
H69	4.4395621136	-2.1865898780	-1.4513885892
C70	0.3219934928	-0.0074883445	-1.4398581731
H71	-0.1567420856	-0.8887675048	-1.8838010011
H72	-0.1386776259	0.8783372817	-1.8932579159
N73	9.8530377239	-3.0557369620	4.8631575412
N74	9.8000656938	3.5186778782	2.1967494443
N75	3.3479448047	-3.2320947708	4.6850346774
N76	3.2696542308	3.4830693114	2.4000952500
C77	9.9626734582	-2.8414431791	3.5154798014
H78	10.0757668258	-3.7320398920	2.9018716356
C79	9.9644420354	-1.5907449159	2.9838202073
H80	10.0945217228	-1.5131607303	1.9088681101
C81	9.8559583074	-0.4250735346	3.8034093181
C82	9.7748780000	-0.6925926484	5.2042443007
H83	9.7061376333	0.1122494381	5.9307738901
C84	9.7596985192	-1.9661851736	5.6853177409
H85	9.6771706878	-2.1846872932	6.7479792080
C86	9.8523218156	0.8918688976	3.2656638378
C87	9.8333812499	1.1563836559	1.8625017512
H88	9.8330450327	0.3481430647	1.1358451749
C89	9.7881878678	2.4257980444	1.3750157488
H90	9.7473079568	2.6374656258	0.3085653657
C91	9.8646831952	3.3104458616	3.5487148141
H92	9.9224358724	4.2059347501	4.1626562366
C93	9.8888806344	2.0617174442	4.0851474560
H94	9.9807659525	1.9891452282	5.1645122013
C95	9.4331331588	4.8468561581	1.6723312872
H96	9.9258200800	5.6006486098	2.2984734910
H97	9.8487985440	4.9388320584	0.6619319770
C98	7.9332754646	4.9987123437	1.6825755383
C99	7.1741222808	4.7558965319	0.5391754113
H100	7.6739322969	4.5769098744	-0.4142431599
C101	5.7829631265	4.7501802309	0.6022758243
H102	5.2023609200	4.5702803220	-0.3046278707
C103	5.1262820595	4.9788318189	1.8108554857

C104	5.8872169835	5.2756088543	2.9433407577
H105	5.3904183183	5.5125803728	3.8851664188
C106	7.2729111924	5.2894155765	2.8787946789
H107	7.8482808715	5.5392313497	3.7705283130
C108	3.6315404446	4.8342365409	1.9274693888
H109	3.1333112275	4.9955462457	0.9633924912
H110	3.2094658215	5.5561967285	2.6371654012
C111	3.1964813263	3.2011449773	3.7404056035
H112	3.1857202116	4.0652971472	4.4010643969
C113	3.1354062251	1.9252769141	4.2099816053
H114	3.0692789082	1.7944703204	5.2870937450
C115	3.1587462629	0.7984601335	3.3222175098
C116	3.1969446980	1.1410165994	1.9360511442
H117	3.2030093518	0.3819283891	1.1561684732
C118	3.2671961911	2.4362587250	1.5226046313
H119	3.3260308001	2.6965047109	0.4661796304
C120	3.1716358943	-0.5453581138	3.7799136564
C121	3.2092585592	-0.8920100448	5.1656882289
H122	3.1873673453	-0.1367071747	5.9494372530
C123	3.3142990889	-2.1899298678	5.5691390927
H124	3.3777030891	-2.4568654433	6.6236696069
C125	3.2733498026	-2.9436245575	3.3454026768
H126	3.2849748978	-3.8032108300	2.6788520782
C127	3.1824237246	-1.6676929038	2.8850444768
H128	3.1169065362	-1.5328082956	1.8085193295
C129	3.7422190044	-4.5796735237	5.1418880825
H130	3.2566540047	-4.7614134540	6.1087306432
H131	3.3285616732	-5.3032335130	4.4285379935
C132	5.2405193339	-4.6940012081	5.2455078641
C133	5.8955805472	-4.4953141325	6.4592287156
H134	5.3138823544	-4.3696121322	7.3744726642
C135	7.2865997998	-4.4557163681	6.5157739155
H136	7.7857722826	-4.2981765468	7.4732186666
C137	8.0470788897	-4.6187361880	5.3594652496
C138	7.3904441577	-4.8888973341	4.1558853769
H139	7.9687215348	-5.0807439562	3.2515418892
C140	6.0048815146	-4.9241439992	4.0994072434
H141	5.5114400649	-5.1435318959	3.1514209512
C142	9.5391855689	-4.4038289014	5.3716496014
H143	10.0644285699	-5.1280826119	4.7370642421
H144	9.9569483390	-4.4923628845	6.3815189372

$HC^{4(\bullet+)}$	**X**	**Y**	**Z**
N1	0.0000000000	0.0000000000	0.0000000000

N2	0.0000000000	0.0000000000	7.0828006111
N3	6.4861215075	0.0000000000	-0.0174348969
N4	6.5306552001	0.0182645152	7.0919505433
C5	-0.0541978354	-1.1722185353	0.6903031814
H6	-0.1009621759	-2.0769025238	0.0891055287
C7	-0.0767115078	-1.2021213333	2.0553232232
H8	-0.1638590787	-2.1760729223	2.5268723876
C9	-0.0344305173	-0.0040570304	2.8207796799
C10	-0.0218128889	1.1930403447	2.0609148658
H11	-0.0322895345	2.1695374124	2.5362200867
C12	0.0071158020	1.1690162914	0.6937230126
H13	0.0222903172	2.0783692805	0.0970967895
C14	-0.0384518486	-0.0024473815	4.2620592211
C15	-0.0078198672	-1.1974348684	5.0239942351
H16	-0.0034086705	-2.1742878565	4.5502795323
C17	0.0250785089	-1.1698164174	6.3911283385
H18	0.0593305980	-2.0772777761	6.9899182875
C19	-0.0831162503	1.1702520763	6.3901837868
H20	-0.1517037347	2.0752120782	6.9892477598
C21	-0.1075863470	1.1958217529	5.0251757367
H22	-0.2186308683	2.1660718743	4.5524193855
C23	0.3328832120	0.0110595616	8.5298113475
H24	-0.1392807738	0.8960898963	8.9715344818
H25	-0.1285987928	-0.8707855778	8.9883879264
C26	1.8325273724	0.0221617759	8.6820885794
C27	2.5463465151	-1.1644005346	8.8473603164
H28	2.0116492784	-2.1018041010	9.0074175768
C29	3.9383099786	-1.1584243014	8.8358152690
H30	4.4824780801	-2.0922640934	8.9880784224
C31	4.6419574379	0.0323561292	8.6589685387
C32	3.9266506916	1.2274072113	8.5512675064
H33	4.4590911993	2.1770346589	8.4825554439
C34	2.5376104348	1.2226701056	8.5621986843
H35	1.9974325359	2.1685721131	8.5007276752
C36	6.1419307829	0.0341118703	8.5185663192
H37	6.5954474345	-0.8406937050	9.0000644188
H38	6.5923303225	0.9245207273	8.9739671543
C39	6.6207088706	1.1878851843	6.3829397549
H40	6.6372591374	2.0981583650	6.9785382504
C41	6.6884396723	1.2074242018	5.0239982982
H42	6.7601154642	2.1828898921	4.5474646479
C43	6.6594683953	0.0007692982	4.2462376225
C44	6.6131333872	-1.1949922077	5.0326649206
H45	6.6121245765	-2.1844391354	4.5776905423
C46	6.5367526563	-1.1545891161	6.3923173073
H47	6.4675903115	-2.0643302409	6.9882928352

C48	6.6386346983	0.0006140102	2.8269089871
C49	6.6152603724	1.2010541572	2.0470605897
H50	6.6425640171	2.1873177472	2.5097719856
C51	6.5305892284	1.1694713976	0.6867083615
H52	6.4878134721	2.0849138100	0.0965074201
C53	6.5249421889	-1.1754248801	0.6877431087
H54	6.4962961380	-2.0827153485	0.0887840789
C55	6.5986228949	-1.2033892055	2.0453695036
H56	6.6256057010	-2.1820918164	2.5185696881
C57	6.1165972350	0.0003810169	-1.4492128252
H58	6.5741157877	0.8828312618	-1.9124645241
H59	6.5748518561	-0.8823100726	-1.9104987484
C60	4.6190890868	-0.0008265770	-1.6068655992
C61	3.9106960103	1.1957155864	-1.7193168330
H62	4.4519898651	2.1386682803	-1.8208658921
C63	2.5192271215	1.1959965731	-1.7262484888
H64	1.9798306819	2.1381506887	-1.8352337114
C65	1.8116528222	-0.0020892360	-1.6206776106
C66	2.5209440080	-1.2035597159	-1.5720200464
H67	1.9843859933	-2.1530704603	-1.5602944089
C68	3.9098540163	-1.2027522890	-1.5671995073
H69	4.4469302317	-2.1517245269	-1.5535133746
C70	0.3146500037	-0.0014836141	-1.4515401461
H71	-0.1572724622	-0.8863964732	-1.8931612680
H72	-0.1581015580	0.8804079155	-1.8983486906
N73	9.7292678458	-3.4798021854	4.4998001572
N74	9.8258102776	3.2759493419	2.3800323897
N75	3.2447103553	-3.3941856759	4.5355008855
N76	3.3290538613	3.4275829699	2.5633908325
C77	9.7353133585	-3.1705074469	3.1736311001
H78	9.7455544802	-4.0146557695	2.4889494338
C79	9.7551032217	-1.8771721741	2.7359428752
H80	9.8064462906	-1.7195425265	1.6641822477
C81	9.7687501087	-0.7900782528	3.6536599112
C82	9.8001511409	-1.1581266782	5.0229822436
H83	9.8541600784	-0.4134016117	5.8124017057
C84	9.7682662867	-2.4698884789	5.4087635749
H85	9.7893773460	-2.7684676792	6.4544555427
C86	9.7888854949	0.5854599236	3.2251524938
C87	9.7453039333	0.9529137101	1.8560949055
H88	9.7101892821	0.2085695079	1.0661196025
C89	9.7500140131	2.2662859277	1.4734152008
H90	9.7096408809	2.5668771014	0.4286174733
C91	9.9120428597	2.9640792899	3.7042553043
H92	10.0185211543	3.8047869167	4.3857269886
C93	9.8951272838	1.6701377274	4.1407996119

H94	10.0119281607	1.5077943855	5.2071162019
C95	9.5339778287	4.6704244567	1.9602397588
H96	10.0499761722	5.3416447072	2.6565165186
H97	9.9748540515	4.8235356620	0.9686125420
C98	8.0398147529	4.8700450940	1.9661370883
C99	7.2878409636	4.7315226375	0.7998628691
H100	7.7923943777	4.6227265124	-0.1616179465
C101	5.8956389327	4.7517042662	0.8513041519
H102	5.3215562498	4.6615864052	-0.0728014709
C103	5.2319342690	4.9048803683	2.0686004278
C104	5.9876907799	5.1098096257	3.2257535406
H105	5.4877239621	5.3064023999	4.1752172878
C106	7.3748801950	5.0943343539	3.1750000666
H107	7.9465062924	5.2787221758	4.0855367431
C108	3.7317900378	4.7931860612	2.1609893411
H109	3.2496516827	5.0140991099	1.2008288087
H110	3.3179200674	5.4910144081	2.8990493358
C111	3.2379857587	3.0808906398	3.8876435132
H112	3.2527296622	3.9111261790	4.5907326827
C113	3.1312868328	1.7854890346	4.2946927707
H114	3.0648958009	1.6068398825	5.3665192210
C115	3.1213455900	0.7002945235	3.3529697908
C116	3.1674121192	1.1141090437	1.9828019938
H117	3.1417796196	0.3960668733	1.1636252957
C118	3.2827013514	2.4260839259	1.6355252925
H119	3.3526299443	2.7381149513	0.5933603199
C120	3.1126956799	-0.6625171450	3.7451704980
C121	3.1476223495	-1.0769871953	5.1149973723
H122	3.1416373339	-0.3569629711	5.9325201180
C123	3.2216031732	-2.3917268248	5.4633057819
H124	3.2746584275	-2.7042814749	6.5060138367
C125	3.1849254310	-3.0447607979	3.2103316165
H126	3.1941593084	-3.8747682934	2.5069915110
C127	3.1151644806	-1.7476443400	2.8036928174
H128	3.0704347245	-1.5676633681	1.7322046040
C129	3.6029973286	-4.7722878188	4.9363728785
H130	3.1412447959	-4.9647514555	5.9123533858
H131	3.1404133717	-5.4593786995	4.2176182348
C132	5.0989515247	-4.9406427412	4.9841551827
C133	5.8109256153	-4.6889506915	6.1578971444
H134	5.2730706464	-4.4861220363	7.0861855800
C135	7.2018517521	-4.7189288902	6.1626999881
H136	7.7438605066	-4.5375246191	7.0923675891
C137	7.9061137477	-5.0048645304	4.9927622307
C138	7.1927878099	-5.3218199908	3.8356351475
H139	7.7253721138	-5.6175388430	2.9311309557

C140	5.8040131316	-5.2894984221	3.8311505152
H141	5.2634373798	-5.5605187532	2.9236098015
C142	9.4049061321	-4.8611342159	4.9402115191
H143	9.8691254078	-5.5557861480	4.2311726562
H144	9.8784366027	-5.0209822266	5.9154617734

$HC^{3\bullet 5+}$	**X**	**Y**	**Z**
N1	0.0000000000	0.0000000000	0.0000000000
N2	0.0000000000	0.0000000000	7.0532337949
N3	6.5416218685	0.0000000000	0.0783982990
N4	6.5561893280	-0.4293611460	7.1670974723
C5	0.0954408087	-1.1632929219	0.6879675766
H6	0.2300748676	-2.0639909689	0.0929289801
C7	0.0305772509	-1.1909079070	2.0595146923
H8	0.1312787836	-2.1567463472	2.5497684193
C9	-0.1175524801	0.0015703593	2.7955277456
C10	-0.2692379306	1.1860638637	2.0426243776
H11	-0.4852842237	2.1403271878	2.5154648737
C12	-0.2088365565	1.1584921872	0.6709147214
H13	-0.3395649205	2.0524090372	0.0646144118
C14	-0.1174199123	0.0074309860	4.2571896270
C15	-0.3532724152	-1.1640547419	5.0099926610
H16	-0.6375979294	-2.1003639925	4.5364599745
C17	-0.2916981968	-1.1411025519	6.3813519556
H18	-0.4908749376	-2.0228923169	6.9872826400
C19	0.1772645687	1.1534551661	6.3652772054
H20	0.3743172627	2.0425380613	6.9606333565
C21	0.1120096539	1.1866160125	4.9937896960
H22	0.2734509123	2.1446790327	4.5045078240
C23	0.3271376496	-0.0434423041	8.5117939320
H24	-0.0647265552	0.8727039681	8.9687764726
H25	-0.2216403388	-0.8890093661	8.9438302616
C26	1.8229874755	-0.1750126982	8.6670411346
C27	2.4411520591	-1.4035294650	8.4115123902
H28	1.8360532010	-2.2947294456	8.2322462680
C29	3.8259760044	-1.5114469282	8.4230277574
H30	4.2885171330	-2.4862090050	8.2547459939
C31	4.6261943303	-0.3950170838	8.6913891903
C32	4.0075420757	0.8134103753	9.0119958704
H33	4.6127166276	1.6758650608	9.3007731637
C34	2.6159581186	0.9246167378	8.9978369855
H35	2.1478226222	1.8711963455	9.2752487512
C36	6.1277566409	-0.5092634510	8.5859631987
H37	6.4863912251	-1.4663387959	8.9835357434

H38	6.6419293332	0.2859846272	9.1387371024
C39	6.6691139290	0.7803090617	6.5456790356
H40	6.6500685234	1.6556064817	7.1935395463
C41	6.7983898637	0.8981527198	5.1906571397
H42	6.8846463597	1.9099845884	4.7960922299
C43	6.7773109390	-0.2471015329	4.3363741865
C44	6.7300494959	-1.4964416908	5.0372443810
H45	6.7815043982	-2.4431893890	4.5046910968
C46	6.6130926091	-1.5556915391	6.3932922015
H47	6.5641443790	-2.4994447668	6.9316536353
C48	6.7677021871	-0.1603055007	2.9125863586
C49	6.7839388327	1.0850958841	2.1976985309
H50	6.8947731968	2.0352512346	2.7184495999
C51	6.6628240067	1.1328360812	0.8403458983
H52	6.6687575986	2.0713053158	0.2891493442
C53	6.5734121369	-1.2066255713	0.7160615324
H54	6.4947857214	-2.0874200675	0.0787173493
C55	6.7025362225	-1.3140820605	2.0713962489
H56	6.7280585782	-2.3256961482	2.4808761139
C57	6.1504647804	0.0813958005	-1.3512387191
H58	6.5988443115	0.9931757000	-1.7646138892
H59	6.6097189583	-0.7675635835	-1.8716929600
C60	4.6504689213	0.0754187974	-1.5031528344
C61	3.9252696856	1.2583498869	-1.3369217812
H62	4.4494106837	2.2069583392	-1.2110578005
C63	2.5367772850	1.2451555308	-1.3734187297
H64	1.9894346482	2.1836966442	-1.2716242382
C65	1.8443272217	0.0486046820	-1.5797957840
C66	2.5663724918	-1.1231517399	-1.8055817609
H67	2.0421089881	-2.0510472701	-2.0410468541
C68	3.9598270460	-1.1071808705	-1.7694393940
H69	4.5131045358	-2.0248976688	-1.9794658993
C70	0.3415457437	0.0210875750	-1.4561705604
H71	-0.1086722029	-0.8652935656	-1.9177258270
H72	-0.1404224255	0.9029590090	-1.8940048390
N73	10.0622252093	-3.6479783484	2.1691962903
N74	10.3526735750	2.8394346277	4.9419473611
N75	3.5316500838	-3.4391095159	2.4715393911
N76	3.8451299369	3.2850960179	4.7290197563
C77	9.9625204667	-2.5549167066	1.3763066566
H78	9.7806999714	-2.7431825314	0.3208838632
C79	10.0816391269	-1.2840603348	1.8870645958
H80	9.9803451157	-0.4519479366	1.1943876141
C81	10.2863595755	-1.0796289445	3.2656118072
C82	10.4404578634	-2.2432318052	4.0508812299
H83	10.6980648183	-2.1908337443	5.1048540836

C84	10.3286442197	-3.4917960393	3.4886610021
H85	10.4618062979	-4.4043048213	4.0661186241
C86	10.3409927290	0.2622074068	3.8463973771
C87	10.5615980465	1.4106756437	3.0529042184
H88	10.7856876266	1.3389198498	1.9920427009
C89	10.5678909260	2.6632359482	3.6158585128
H90	10.7601535851	3.5622566869	3.0327964987
C91	10.1774377402	1.7570425755	5.7400795710
H92	10.0355796299	1.9581044389	6.7996661863
C93	10.1799430868	0.4816220479	5.2290783055
H94	10.0192071664	-0.3403198084	5.9244559854
C95	10.0963318251	4.2084873801	5.4886836458
H96	10.5174938631	4.2459424671	6.4999238550
H97	10.6583199423	4.9190070910	4.8700133126
C98	8.6081910758	4.4626542201	5.4652253763
C99	7.9773268406	4.8119493078	4.2669861769
H100	8.5726286655	5.0460941157	3.3830449567
C101	6.5911030840	4.9004670212	4.1980876518
H102	6.1198028216	5.2044461980	3.2619367426
C103	5.8057965979	4.6414153763	5.3252191721
C104	6.4404737402	4.3637658033	6.5362495027
H105	5.8519063499	4.2312084094	7.4460573976
C106	7.8302536007	4.2724416964	6.6070465536
H107	8.3105610302	4.0757318489	7.5673487183
C108	4.3020233908	4.6118466333	5.2116373970
H109	3.9267479627	5.3677208708	4.5107473444
H110	3.8178542277	4.7995390589	6.1766095340
C111	3.6898588562	2.2533150733	5.6056611196
H112	3.7192218850	2.5148100776	6.6624429001
C113	3.5050455398	0.9655285034	5.1916587101
H114	3.3805113819	0.2135729781	5.9704596214
C115	3.5085954270	0.6164972279	3.8092329501
C116	3.6157944282	1.7371823292	2.9219933488
H117	3.5681862192	1.6129374845	1.8427503193
C118	3.7860679121	3.0061124476	3.3911691048
H119	3.8781717972	3.8637830328	2.7289898726
C120	3.4496423830	-0.7381115038	3.3594059903
C121	3.4100681999	-1.8535347583	4.2588880429
H122	3.3394836461	-1.7120014671	5.3347169264
C123	3.4609545144	-3.1395364697	3.8043543268
H124	3.4387153041	-3.9946586331	4.4762892893
C125	3.5167433296	-2.4055884233	1.5817180255
H126	3.5539260619	-2.6822169224	0.5290381996
C127	3.4604881757	-1.0990857563	1.9782687122
H128	3.4475801358	-0.3494658821	1.1881090508
C129	3.8643387326	-4.8130430054	2.0115454006

H130	3.4371280744	-5.5166008208	2.7355591404
H131	3.3498629598	-4.9795212807	1.0587911772
C132	5.3565987909	-4.9827321148	1.8750822224
C133	6.1355007025	-5.2436793824	3.0041566561
H134	5.6563710944	-5.4398649556	3.9637680831
C135	7.5193519981	-5.2946780494	2.9097796473
H136	8.1067548868	-5.5299936857	3.7971742209
C137	8.1570582464	-5.0816545215	1.6849376596
C138	7.3786605650	-4.8900382107	0.5458053776
H139	7.8554562028	-4.7997208483	-0.4309958336
C140	5.9890964006	-4.8425136476	0.6413012987
H141	5.3937303013	-4.7171554194	-0.2637451235
C142	9.6618181304	-4.9879241747	1.6370391900
H143	10.0647556257	-5.0803747613	0.6230475354
H144	10.1533497177	-5.7467722702	2.2563522236

$HC^{2\bullet 6+}$	**X**	**Y**	**Z**
N1	0.0000000000	0.0000000000	0.0000000000
N2	0.0000000000	0.0000000000	6.9378763981
N3	6.8965161580	0.0000000000	-0.0686040607
N4	6.8918667982	-0.4453571283	6.9558166170
C5	0.1816448747	-1.1251635447	0.7217237960
H6	0.5610877096	-1.9883865750	0.1820967956
C7	-0.0711220198	-1.1501123229	2.0750522804
H8	0.1237749455	-2.0687932357	2.6227566076
C9	-0.5076285714	0.0104861577	2.7277993322
C10	-0.7891136926	1.1308023576	1.9387001700
H11	-1.2167231573	2.0384171254	2.3615792719
C12	-0.5274573391	1.0980616335	0.5786955376
H13	-0.7177649197	1.9511053102	-0.0702899358
C14	-0.5111141403	0.0449931879	4.2122253637
C15	-0.8664448421	-1.0597403956	4.9931956830
H16	-1.3513031115	-1.9341115401	4.5628556732
C17	-0.6016280633	-1.0554525735	6.3523100895
H18	-0.8451254170	-1.8996656464	6.9946619855
C19	0.2486336884	1.1183257183	6.2261834479
H20	0.6865040120	1.9495492775	6.7722830334
C21	-0.0052038876	1.1716766894	4.8735152988
H22	0.2469586708	2.0808615758	4.3326154478
C23	0.5122779064	-0.0781628822	8.3551442590
H24	0.1560699276	0.8179398882	8.8767245566
H25	0.0267021056	-0.9432089883	8.8203646680
C26	2.0198440464	-0.1880162433	8.3581983291
C27	2.6397288246	-1.3986098800	8.0314075678

H28	2.0360420300	-2.2834679617	7.8231815892
C29	4.0251422010	-1.5051741157	8.0317846624
H30	4.4847934816	-2.4759103540	7.8337708436
C31	4.8297423914	-0.4041701333	8.3482459617
C32	4.2089537922	0.7933783811	8.7032892685
H33	4.8085443586	1.6445021164	9.0300625673
C34	2.8176227345	0.9007435509	8.7097042116
H35	2.3584835208	1.8324897347	9.0411174242
C36	6.3379387795	-0.5265418988	8.3345083626
H37	6.6677101042	-1.4807856859	8.7626756562
H38	6.8062307287	0.2677747619	8.9269477365
C39	7.0657547354	0.7647933389	6.3513933152
H40	6.9805055880	1.6351676583	7.0009655752
C41	7.3185509767	0.8783069145	5.0120668808
H42	7.4363248034	1.8890708776	4.6206779179
C43	7.3659004022	-0.2665370851	4.1607157066
C44	7.3371229602	-1.5091062731	4.8639906841
H45	7.4960260793	-2.4525177574	4.3466059084
C46	7.0828939196	-1.5695667749	6.2047582973
H47	7.0236025994	-2.5145522747	6.7428186284
C48	7.3668844784	-0.1802170818	2.7278568659
C49	7.3122213083	1.0648372946	2.0291271315
H50	7.4452813245	2.0111686796	2.5488693666
C51	7.0616610393	1.1250461263	0.6884457824
H52	6.9845512673	2.0713509152	0.1544515097
C53	7.0963535199	-1.2093045201	0.5325199389
H54	7.0320493132	-2.0790813595	-0.1201430445
C55	7.3523164369	-1.3228863603	1.8715450955
H56	7.4966435028	-2.3320571001	2.2610494496
C57	6.3402591730	0.0859665181	-1.4454730197
H58	6.7266498653	1.0078778447	-1.8971991765
H59	6.7544808058	-0.7492981156	-2.0214466030
C60	4.8271678611	0.0614771436	-1.4534302907
C61	4.0993481162	1.2277212381	-1.1891927631
H62	4.6219327885	2.1744090963	-1.0373058931
C63	2.7097456308	1.2128594609	-1.1791841415
H64	2.1662895366	2.1439919974	-1.0093476958
C65	2.0094765035	0.0322815553	-1.4464578433
C66	2.7307268826	-1.1223455031	-1.7534214276
H67	2.2073342747	-2.0347107871	-2.0427391869
C68	4.1260446766	-1.1072841837	-1.7538026582
H69	4.6673753111	-2.0093838306	-2.0433313604
C70	0.4986474730	0.0264560957	-1.4240755357
H71	0.0743146249	-0.8488891263	-1.9286521267
H72	0.0680788491	0.9174590108	-1.8946722574
N73	11.6490522361	-3.4705184308	2.4349161313

N74	11.5280037941	3.3034471535	3.9644884298
N75	4.7810037379	-3.7795234787	2.8704520697
N76	4.6344343306	3.1763013832	3.9533100885
C77	11.3573503025	-2.5317956081	1.5107418614
H78	10.9173793336	-2.8890964033	0.5828610349
C79	11.5757363315	-1.1952756097	1.7629622964
H80	11.2934637306	-0.4700167326	1.0034194018
C81	12.0902396318	-0.7909094517	3.0022565292
C82	12.4813695207	-1.7903506796	3.8988736742
H83	12.9700031688	-1.5552700800	4.8427959295
C84	12.2515828708	-3.1208557594	3.5894666766
H85	12.5262867977	-3.9297728836	4.2640424171
C86	12.0668036352	0.6496421142	3.3621508572
C87	12.3278495979	1.6654030644	2.4364327163
H88	12.7506272646	1.4528173389	1.4559033318
C89	12.0509823288	2.9824503804	2.7635019632
H90	12.2237732549	3.8023622270	2.0686322549
C91	11.3688208822	2.3544155471	4.9102058526
H92	10.9922227519	2.6911146818	5.8730910678
C93	11.6380590189	1.0307951176	4.6404858779
H94	11.4608994534	0.2951955506	5.4211635095
C95	10.9974170750	4.6887216421	4.2414061157
H96	11.4088081566	5.0052782240	5.2069844918
H97	11.4164845634	5.3487466789	3.4736335700
C98	9.4862251975	4.6722313249	4.2308117448
C99	8.7931124014	4.6263727994	3.0169332345
H100	9.3400341103	4.6635409713	2.0732272113
C101	7.4039316650	4.5967286954	2.9970908424
H102	6.8854442760	4.6219708647	2.0362673286
C103	6.6691558270	4.5987914416	4.1888581568
C104	7.3623165750	4.6786311104	5.3973812799
H105	6.8135151199	4.7640346407	6.3366340835
C106	8.7571726828	4.7175282168	5.4194273537
H107	9.2724244117	4.8319448370	6.3741044863
C108	5.1565517499	4.5546323580	4.1566390756
H109	4.7585809103	5.1762140758	3.3450510778
H110	4.7277084876	4.9375550933	5.0903666229
C111	4.4735272037	2.3242969146	5.0085421301
H112	4.5454372626	2.7757776632	5.9975124339
C113	4.2452129974	0.9860187294	4.8361701045
H114	4.1341558786	0.3851311946	5.7406349880
C115	4.2217670138	0.3941696398	3.5365554133
C116	4.2373886287	1.3449503231	2.4702267749
H117	4.0964642032	1.0377510375	1.4362527540
C118	4.4608700311	2.6729190395	2.6945812238
H119	4.5087197000	3.3980783411	1.8830938546

C120	4.2519237712	-1.0233698426	3.3115639297
C121	4.3178747389	-1.9789824231	4.3708537580
H122	4.1656017756	-1.6827549573	5.4063054620
C123	4.5970583920	-3.2954986176	4.1335796572
H124	4.6832874998	-4.0248234906	4.9376488903
C125	4.5721690599	-2.9306021373	1.8239527641
H126	4.6513996505	-3.3732043635	0.8317635597
C127	4.2926310126	-1.6047077542	2.0088872356
H128	4.1458613840	-1.0062629226	1.1094437775
C129	5.3651136731	-5.1296709416	2.6416740910
H130	5.0549566103	-5.7650418196	3.4799430144
H131	4.9011571505	-5.5444695298	1.7389535478
C132	6.8724041119	-5.0779470280	2.5143678164
C133	7.6761405614	-4.9917833028	3.6573700682
H134	7.2188084481	-5.0252846708	4.6486548829
C135	9.0598734607	-4.9286353629	3.5513959086
H136	9.6649091388	-4.9031616345	4.4592308533
C137	9.6788362859	-4.9616906644	2.2974742959
C138	8.8838421294	-5.0859067950	1.1582214945
H139	9.3464998090	-5.1890440613	0.1756079530
C140	7.4933881974	-5.1415931673	1.2667379048
H141	6.8955504180	-5.2880784148	0.3658430506
C142	11.1842793554	-4.8858013612	2.1917066521
H143	11.5521587517	-5.1806318918	1.2019425198
H144	11.6900708464	-5.5165019439	2.9313028008

$HC^{\bullet 7+}$	**X**	**Y**	**Z**
N1	0.0000000000	0.0000000000	0.0000000000
N2	0.0000000000	0.0000000000	6.9198181023
N3	7.0351773165	0.0000000000	-0.0071812836
N4	7.0280012570	-0.3490885234	6.9647425709
C5	0.0726024633	-1.1475472040	0.7077592615
H6	0.3966717613	-2.0323867050	0.1641208826
C7	-0.2223582159	-1.1725662625	2.0538518148
H8	-0.1139957096	-2.1146423446	2.5864229198
C9	-0.5989297771	0.0054768627	2.7155571107
C10	-0.8114611232	1.1422416858	1.9254235029
H11	-1.2198231867	2.0631897682	2.3387934848
C12	-0.5022233279	1.1136446158	0.5746121146
H13	-0.6335557788	1.9824207107	-0.0687835803
C14	-0.5971179061	0.0398886107	4.2036038131
C15	-0.8946499486	-1.0765732476	4.9938779413
H16	-1.3695160123	-1.9642694545	4.5808205426
C17	-0.5848703170	-1.0719857399	6.3449015928

H18	-0.7813091900	-1.9292027174	6.9871474069
C19	0.1611715749	1.1383240458	6.2116100734
H20	0.5527727430	1.9953808548	6.7558053647
C21	-0.1311083602	1.1853868447	4.8658536096
H22	0.0485907288	2.1157847713	4.3332368520
C23	0.5629871231	-0.0666610462	8.3173042122
H24	0.2020618994	0.8189020807	8.8541147082
H25	0.1151378184	-0.9417712200	8.8019790037
C26	2.0778487963	-0.1424847608	8.2864801356
C27	2.7237112494	-1.3508422849	7.9977054059
H28	2.1377642889	-2.2558391999	7.8290825006
C29	4.1130302320	-1.4344999999	8.0077557007
H30	4.5856510209	-2.4096001378	7.8660222212
C31	4.8998782839	-0.3093902243	8.2902614704
C32	4.2544187505	0.8887956154	8.6042763956
H33	4.8330534190	1.7578312925	8.9228013145
C34	2.8598813844	0.9694125929	8.6056868999
H35	2.3865904879	1.8999120277	8.9202882566
C36	6.4097209019	-0.4147859125	8.3382820262
H37	6.7395767257	-1.3586436205	8.7886324750
H38	6.8539898557	0.3949013271	8.9279734134
C39	7.2552120396	0.8471630569	6.3664321841
H40	7.1427196340	1.7270030275	6.9993819825
C41	7.5788300321	0.9427903940	5.0322608227
H42	7.7229669469	1.9484575545	4.6364205818
C43	7.6542045537	-0.2097439017	4.2119932044
C44	7.5875177844	-1.4361530264	4.9145666348
H45	7.7550526022	-2.3905514273	4.4162648612
C46	7.2654756378	-1.4784617570	6.2515230933
H47	7.1690164681	-2.4173082287	6.7961774359
C48	7.6557577064	-0.1405830125	2.7466324987
C49	7.5427004381	1.0891939166	2.0543112481
H50	7.6634150242	2.0456764846	2.5627414294
C51	7.2263686167	1.1310913088	0.7172680342
H52	7.0967947487	2.0704647710	0.1806436100
C53	7.3071325345	-1.1917971331	0.5815324325
H54	7.2336449430	-2.0696880283	-0.0598000418
C55	7.6311033792	-1.2877878688	1.9165662836
H56	7.8158556319	-2.2906803203	2.3048519633
C57	6.4264253346	0.0658341763	-1.3856205222
H58	6.8085712842	0.9798117773	-1.8560706442
H59	6.8315938492	-0.7800182382	-1.9519710330
C60	4.9121146849	0.0428723530	-1.3497412085
C61	4.1842052731	1.2256332869	-1.1634562736
H62	4.7053559280	2.1827003316	-1.0911832978
C63	2.7917930391	1.2148332161	-1.1629405153

H64	2.2527419662	2.1591505361	-1.0704475482
C65	2.0851895563	0.0236872547	-1.3649543768
C66	2.8091517005	-1.1482408475	-1.5977739687
H67	2.2873229110	-2.0718480819	-1.8519449144
C68	4.2057600129	-1.1402978747	-1.5855284140
H69	4.7413755891	-2.0580151424	-1.8360275364
C70	0.5685167171	0.0250661763	-1.3973037615
H71	0.1637521873	-0.8465552422	-1.9244841367
H72	0.1660195442	0.9161400739	-1.8923817827
N73	12.1547689156	-3.4277582617	2.9135078574
N74	11.8520638549	3.4046187898	3.9766579851
N75	5.1234279003	-3.8128006266	3.0474421701
N76	4.8313257681	3.1190084340	3.8426631339
C77	12.0154665161	-2.5592619085	1.8894035296
H78	11.6884825559	-2.9786027844	0.9402193133
C79	12.2478151599	-1.2119985804	2.0633887505
H80	12.0867718712	-0.5492936413	1.2163075517
C81	12.6304028327	-0.7183278616	3.3192687244
C82	12.9116819739	-1.6596375212	4.3172326553
H83	13.3279377301	-1.3710626204	5.2811201447
C84	12.6629624440	-3.0040970618	4.0902919977
H85	12.8479367087	-3.7637989204	4.8483026674
C86	12.5653567380	0.7455149203	3.5802375121
C87	12.7758145547	1.7076538575	2.5846443757
H88	13.2270296037	1.4557484488	1.6262147800
C89	12.4081566436	3.0253758984	2.8062127554
H90	12.5352875855	3.7974382917	2.0488464667
C91	11.7766480505	2.5272129047	5.0002724121
H92	11.4049797852	2.9169066354	5.9455090302
C93	12.1264116186	1.2050465551	4.8308355875
H94	12.0132102097	0.5309362453	5.6767080639
C95	11.2272887492	4.7675408932	4.1448982733
H96	11.5985032501	5.1785364704	5.0913965141
H97	11.6201005581	5.4020736077	3.3422576606
C98	9.7132679392	4.6755696254	4.1121936262
C99	9.0313157713	4.6063555359	2.8919046592
H100	9.5860527921	4.6614148865	1.9537732239
C101	7.6403182801	4.5522771121	2.8555039209
H102	7.1348440477	4.5870438883	1.8874349600
C103	6.8894063562	4.5453071354	4.0382503724
C104	7.5693947322	4.6480842945	5.2548354610
H105	7.0116985049	4.7490441395	6.1878702560
C106	8.9635468086	4.7178526102	5.2903502373
H107	9.4591899345	4.8676647456	6.2497796461
C108	5.3758692463	4.5169154215	3.9942180130
H109	4.9829124355	5.1010732872	3.1533951335

H110	4.9364891137	4.9346860610	4.9075588675
C111	4.6407726792	2.3238104188	4.9271577059
H112	4.7284594169	2.8103837073	5.8983317625
C113	4.3787026910	0.9780284534	4.8070918383
H114	4.2611025549	0.4154079418	5.7347298494
C115	4.3336628309	0.3523656826	3.5364840242
C116	4.3616948858	1.2462074283	2.4386901312
H117	4.2167984177	0.9045488856	1.4142152172
C118	4.6218167170	2.5847660042	2.6125239464
H119	4.6883861604	3.2755378184	1.7723107205
C120	4.3920037738	-1.1027105557	3.3623803309
C121	4.4961455444	-1.9929971460	4.4570885933
H122	4.3162125675	-1.6621362385	5.4789383257
C123	4.8655688494	-3.3065170748	4.2786889738
H124	4.9866564524	-3.9949404341	5.1145471478
C125	4.8617784859	-3.0375519874	1.9663675380
H126	4.9904655899	-3.5138497823	0.9948412115
C127	4.4851915890	-1.7194279339	2.0915521324
H128	4.3108340517	-1.1707380765	1.1655014075
C129	5.8021303859	-5.1504758655	2.8888906276
H130	5.4749908445	-5.7723601956	3.7307969776
H131	5.4013393558	-5.6084896831	1.9771498193
C132	7.3102516024	-5.0173439291	2.8384112868
C133	8.0557869821	-4.9101409648	4.0203317392
H134	7.5546777302	-4.9652434575	4.9899215499
C135	9.4447971689	-4.8310022152	3.9838744922
H136	10.0002553022	-4.8059813494	4.9228776818
C137	10.1323238607	-4.8741535191	2.7651780450
C138	9.3930546966	-5.0152276133	1.5886214076
H139	9.9035102783	-5.1380155218	0.6323655887
C140	7.9978938703	-5.0811457829	1.6237291361
H141	7.4545287688	-5.2594956929	0.6941712291
C142	11.6485944957	-4.8380242893	2.7383055983
H143	12.0574155997	-5.2133658495	1.7925267541
H144	12.0901614809	-5.4394734733	3.5411856193

HC^{8+}	**X**	**Y**	**Z**
N1	0.0000000000	0.0000000000	0.0000000000
N2	0.0000000000	0.0000000000	6.8880403100
N3	7.1551145266	0.0000000000	-0.2602037988
N4	7.1071126263	-0.2141762025	6.6688310447
C5	0.0627532221	-1.1533384993	0.6996335932
H6	0.4018181905	-2.0323825323	0.1557976832
C7	-0.2659232189	-1.1907199160	2.0360676291

H8	-0.1697182899	-2.1390028014	2.5583791370
C9	-0.6739736382	-0.0228944034	2.6989984549
C10	-0.8985455392	1.1090637651	1.9062365013
H11	-1.3462908229	2.0172089522	2.3058889956
C12	-0.5499812227	1.0961117779	0.5647112839
H13	-0.6887088503	1.9650090278	-0.0765710682
C14	-0.6780117049	0.0081857258	4.1881431740
C15	-0.8316358367	-1.1441132104	4.9725418818
H16	-1.2291855936	-2.0722523932	4.5643514715
C17	-0.4794845043	-1.1245713825	6.3106948711
H18	-0.5626782689	-2.0067812022	6.9434128870
C19	-0.0230071188	1.1638526727	6.2021344227
H20	0.2446214721	2.0619811022	6.7545469892
C21	-0.3527711846	1.1938600168	4.8641496045
H22	-0.3205782437	2.1532909434	4.3533895095
C23	0.6220025110	-0.0328353401	8.2593373929
H24	0.2714368867	0.8555725139	8.7971862107
H25	0.2103210380	-0.9020392740	8.7847075006
C26	2.1411436681	-0.0851937650	8.1764428828
C27	2.8199625083	-1.3095029218	8.1630143601
H28	2.2613196118	-2.2417381452	8.2606446735
C29	4.2145080878	-1.3589998464	8.1174352621
H30	4.7079886072	-2.3295278482	8.2050010589
C31	4.9754644276	-0.1829789330	8.0689724971
C32	4.2988285623	1.0411631018	8.1414168079
H33	4.8606503279	1.9729117127	8.2440749645
C34	2.9048093965	1.0884997116	8.1954218157
H35	2.4175666670	2.0549582914	8.3255715427
C36	6.4884966710	-0.2279858007	8.0755705317
H37	6.8708231082	-1.1329656975	8.5615072764
H38	6.9221471698	0.6305103574	8.6012726977
C39	7.4586431904	0.9435381744	6.0703238930
H40	7.4104769190	1.8411357778	6.6863981670
C41	7.8293118633	0.9937036683	4.7354377920
H42	8.0724264215	1.9778650304	4.3266765652
C43	7.8372942733	-0.1707395484	3.9483494551
C44	7.6397946136	-1.3724820771	4.6495397722
H45	7.7058262855	-2.3490495827	4.1701759020
C46	7.2697240722	-1.3646193077	5.9827537865
H47	7.0636483612	-2.2882473793	6.5232931382
C48	7.8592389877	-0.1276786755	2.4499119956
C49	7.8717004361	1.0815914555	1.7406803266
H50	8.1254091455	2.0267931420	2.2258734405
C51	7.5195848684	1.1179385365	0.3984886462
H52	7.4836282596	2.0472738527	-0.1702526264
C53	7.3242980392	-1.1956697889	0.3414020100

H54	7.1207078095	-2.0746700368	-0.2707645431
C55	7.6806983573	-1.2862131816	1.6750631468
H56	7.7613437337	-2.2870544467	2.1012772227
C57	6.4533325213	0.0779631824	-1.6178595287
H58	6.7958612986	1.0078510873	-2.0873382233
H59	6.8392060580	-0.7530785735	-2.2190754237
C60	4.9484989086	0.0300706376	-1.4511242343
C61	4.2342803355	1.1867964239	-1.0989006150
H62	4.7594860597	2.1387609700	-0.9847250821
C63	2.8431769138	1.1772776186	-1.0373781070
H64	2.3156156698	2.1107286896	-0.8368013998
C65	2.1180941303	0.0173331384	-1.3432419988
C66	2.8281851949	-1.1265484510	-1.7136864961
H67	2.2932741222	-2.0184599548	-2.0430793562
C68	4.2262847677	-1.1256009164	-1.7610246974
H69	4.7373286757	-2.0146185007	-2.1333841615
C70	0.5978237866	0.0400176594	-1.3829336326
H71	0.1886684446	-0.8132692757	-1.9373986835
H72	0.2195492482	0.9448933690	-1.8716483206
N73	11.4619392077	-4.3178457385	4.5329835785
N74	12.6343346100	2.4631682416	4.9515098440
N75	4.5922162199	-2.7915495511	3.5382586000
N76	5.7494365196	4.0362189736	3.8001426757
C77	11.8113623224	-3.6111490668	3.4371082917
H78	11.6214138231	-4.0797774352	2.4764282356
C79	12.3626287662	-2.3518962639	3.5461022681
H80	12.5917854899	-1.8144001392	2.6304451107
C81	12.5767566188	-1.7800861425	4.8063411451
C82	12.3847216019	-2.6150609321	5.9152114429
H83	12.6701231578	-2.3121881906	6.9189969889
C84	11.8207143758	-3.8695281310	5.7537898471
H85	11.6336954970	-4.5340673881	6.5948659991
C86	12.8196554529	-0.3143551865	4.9267182605
C87	13.3758788789	0.4594552555	3.9021682231
H88	13.9046094776	0.0136011794	3.0637598839
C89	13.2656544103	1.8415028690	3.9355975512
H90	13.6659978164	2.4732740342	3.1450804168
C91	12.2445687094	1.7514188560	6.0294072620
H92	11.8508059312	2.3208684997	6.8662134279
C93	12.3267694152	0.3764941284	6.0419508058
H94	11.9730414641	-0.1481322459	6.9243239166
C95	12.3041292755	3.9328546985	4.8955476607
H96	12.6481218934	4.3784082590	5.8354288982
H97	12.9133098202	4.3713876893	4.0976496771
C98	10.8211332620	4.1706579110	4.6650987908
C99	10.2658236516	4.0439016800	3.3855416138

H100	10.9032012701	3.7820706099	2.5411206275
C101	8.9309724257	4.3596496398	3.1519960795
H102	8.5694292534	4.3767244401	2.1206936107
C103	8.1024421245	4.7981854831	4.1968355174
C104	8.6567992437	4.9292670937	5.4710079453
H105	8.0738986708	5.3576262022	6.2862940533
C106	10.0010894658	4.6258073298	5.6976164447
H107	10.4199892248	4.8199358898	6.6847057181
C108	6.6821815104	5.2422277507	3.9228918802
H109	6.5857461913	5.8039531304	2.9867613894
H110	6.2758932095	5.8707681008	4.7221868637
C111	5.3053407211	3.4152896710	4.9109863349
H112	5.4822113219	3.9340054466	5.8519972167
C113	4.7147557282	2.1657069936	4.8506878083
H114	4.4170382704	1.7097762574	5.7946232535
C115	4.5755447441	1.4963739916	3.6251705336
C116	4.8585581234	2.2606656696	2.4851757899
H117	4.6597020879	1.8887974063	1.4810141621
C118	5.4417881211	3.5151148369	2.5984351622
H119	5.7102670986	4.1157987661	1.7297880560
C120	4.3385995655	0.0159017648	3.5639373466
C121	4.1983995256	-0.7588024819	4.7275262149
H122	4.0352067736	-0.3161357355	5.7086046159
C123	4.3395545087	-2.1354732643	4.6879798078
H124	4.2836151062	-2.7416833142	5.5908479065
C125	4.5593688007	-2.0933770591	2.3850505445
H126	4.6681058897	-2.6713485647	1.4693408299
C127	4.4257861312	-0.7128843729	2.3668234408
H128	4.4333195823	-0.2277341250	1.3887714844
C129	4.9481702400	-4.2866659295	3.5576254509
H130	4.3305362261	-4.7300166944	4.3456499316
H131	4.5947566386	-4.6904208894	2.6039645742
C132	6.4194847531	-4.5570161525	3.7755111646
C133	6.9317585537	-4.7794015840	5.0588528639
H134	6.2631245655	-4.7984143367	5.9204414362
C135	8.2786912179	-5.0839880973	5.2501832053
H136	8.6309726429	-5.3097265312	6.2563444680
C137	9.1540422405	-5.1923041536	4.1656784263
C138	8.6270982390	-5.0343768359	2.8802336490
H139	9.2496017993	-5.2278735348	2.0085323642
C140	7.2827593361	-4.7201995786	2.6875511850
H141	6.8919284567	-4.6898215008	1.6693561177
C142	10.6162454848	-5.5536267076	4.3738389432
H143	11.0231951651	-6.1212675097	3.5307745978
H144	10.7629086289	-6.1701079143	5.2670256110

Section F. References

1. M. Gomberg, An instance of trivalent carbon: triphenylmethyl. *J. Am. Chem. Soc.* **22**, 757 (1900). doi:10.1021/ja02049a006

2. R. Chiarelli, M. A. Novak, A. Rassat, J. A. Tholence, A ferromagnetic transition at 1.48 K in an organic nitroxide. *Nature* **363**, 147 (1993). doi:10.1038/363147a0

3. A. Rajca, J. Wongsriratanakul, S. Rajca, Magnetic ordering in an organic polymer. *Science* **294**, 1503 (2001). doi:10.1126/science.1065477 Medline

4. S. D. J. McKinnon, B. O. Patrick, A. B. P. Lever, R. G. Hicks, Verdazyl radicals as redox-active, non-innocent, ligands: Contrasting electronic structures as a function of electron-poor and electron-rich ruthenium bis(beta-diketonate) co-ligands. *Chem. Commun.* **46**, 773 (2010). doi:10.1039/b919920a Medline

5. B. D. Koivisto, R. G. Hicks, The magnetochemistry of verdazyl radical-based materials. *Coord. Chem. Rev.* **249**, 2612 (2005). doi:10.1016/j.ccr.2005.03.012

6. A. W. Cordes, R. C. Haddon, R. T. Oakley, Molecular conductors from neutral heterocyclic π-radicals. *Adv. Mater.* **6**, 798 (1994). doi:10.1002/adma.19940061021

7. M. E. Itkis, X. Chi, A. W. Cordes, R. C. Haddon, Magneto-opto-electronic bistability in a phenalenyl-based neutral radical. *Science* **296**, 1443 (2002). doi:10.1126/science.1071372 Medline

8. Y. Morita *et al*., Organic tailored batteries materials using stable open-shell molecules with degenerate frontier orbitals. *Nat. Mater.* **10**, 947 (2011). doi:10.1038/nmat3142 Medline

9. I. Ratera, J. Veciana, Playing with organic radicals as building blocks for functional molecular materials. *Chem. Soc. Rev.* **41**, 303 (2012). doi:10.1039/c1cs15165g Medline

10. L. Michaelis, E. S. Hill, The viologen indicators. *J. Gen. Physiol.* **16**, 859 (1933). doi:10.1085/jgp.16.6.859 Medline

11. L. Michaelis, Semiquinones, the intermediate steps of reversible organic oxidation-reduction. *Chem. Rev.* **16**, 243 (1935). doi:10.1021/cr60054a004

12. E. M. Kosower, J. L. Cotter, Stable free radicals. II. The reduction of 1-methyl-4-cyanopyridinium ion to methylviologen cation radical. *J. Am. Chem. Soc.* **86**, 5524 (1964). doi:10.1021/ja01078a026

13. E. M. Kosower, J. Hajdu, Pyridinyl diradical π-mer. Magnesium iodide complexes. *J. Am. Chem. Soc.* **93**, 2534 (1971). doi:10.1021/ja00739a030

14. S. Hünig, Stable radical ions. *Pure Appl. Chem.* **15**, 109 (1967). doi:10.1351/pac196715010109

15. W.-S. Jeon, H.-J. Kim, C. Lee, K. Kim, Control of the stoichiometry in host-guest complexation by redox chemistry of guests: Inclusion of methylviologen in cucurbit[8]uril. *Chem. Commun.* (17): 1828 (2002). doi:10.1039/b202082c Medline

16. A. C. Fahrenbach *et al*., Solution-phase mechanistic study and solid-state structure of a tris(bipyridinium radical cation) inclusion complex. *J. Am. Chem. Soc.* **134**, 3061 (2012). doi:10.1021/ja2089603 Medline

17. B. Odell *et al*., Cyclobis(paraquat-*p*-phenylene). A tetracationic multipurpose receptor. *Angew. Chem. Int. Ed. Engl.* **27**, 1547 (1988). doi:10.1002/anie.198815471

18. J. M. Spruell *et al*., Highly stable tetrathiafulvalene radical dimers in [3]catenanes. *Nat. Chem.* **2**, 870 (2010). doi:10.1038/nchem.749 Medline

19. A. Coskun *et al*., Mechanically stabilized tetrathiafulvalene radical dimers. *J. Am. Chem. Soc.* **133**, 4538 (2011). doi:10.1021/ja110584c Medline

20. A. Trabolsi *et al*., Radically enhanced molecular recognition. *Nat. Chem.* **2**, 42 (2010). doi:10.1038/nchem.479 Medline

21. L. Hao, X.-D. Zheng, T.-B. Lu, Photoinduced catalytic reaction by a fluorescent active cryptand containing an anthracene fragment. *Angew. Chem. Int. Ed.* **49**, 8148 (2010). doi:10.1002/anie.201004928

22. N. G. Connelly, W. E. Geiger, Chemical redox agents for organometallic chemistry. *Chem. Rev.* **96**, 877 (1996). doi:10.1021/cr940053x Medline

23. W. W. Porter, 3rd, T. P. Vaid, Isolation and characterization of phenyl viologen as a radical cation and neutral molecule. *J. Org. Chem.* **70**, 5028 (2005). doi:10.1021/jo050328g Medline

24. T. M. Bockman, J. K. Kochi, Isolation and oxidation-reduction of methylviologen cation radicals. Novel disproportionation in charge-transfer salts by x-ray crystallography. *J. Org. Chem.* **55**, 4127 (1990). doi:10.1021/jo00300a033

25. D.-L. Sun, S. V. Rosokha, S. V. Lindeman, J. K. Kochi, Intervalence (charge-resonance) transitions in organic mixed-valence systems: Through-space versus through-bond electron transfer between bridged aromatic (redox) centers. *J. Am. Chem. Soc.* **125**, 15950 (2003). doi:10.1021/ja037867s Medline

26. D. Sun, S. V. Rosokha, J. K. Kochi, Donor-acceptor (electronic) coupling in the precursor complex to organic electron transfer: intermolecular and intramolecular self-exchange between phenothiazine redox centers. *J. Am. Chem. Soc.* **126**, 1388 (2004). doi:10.1021/ja038746v Medline

27. S. F. Nelsen, "Almost delocalized" intervalence compounds. *Chemistry* **6**, 581 (2000). doi:10.1002/(SICI)1521-3765(20000218)6:4<581::AID-CHEM581>3.0.CO;2-E Medline

28. P. Neta, M.-C. Richoux, A. Harriman, Intramolecular association of covalently linked viologen radicals. *J. Chem. Soc., Faraday Trans. II* **81**, 1427 (1985). doi:10.1039/f29858101427

29. M. B. Robin, P. Day, Mixed valence chemistry: A survey and classification. *Adv. Inorg. Chem. Radiochem.* **10**, 247 (1968). doi:10.1016/S0065-2792(08)60179-X

30. Jaguar 7.6, Schrödinger, LLC, New York, NY (2006).

31. D. Maspoch *et al*., Carboxylic-substituted polychlorotriphenylmethyl radicals, new organic building-blocks to design nanoporous magnetic molecular materials. *C. R. Chim.* **8**, 1213 (2005). doi:10.1016/j.crci.2005.02.020

32. K. Inoue, H. Iwamura, Ferro- and ferrimagnetic ordering in a two-dimensional network formed by manganese(ii) and 1,3,5-Tris[*p*-(*N*-tert-butyl-*N*-oxyamino)phenyl]benzene. *J. Am. Chem. Soc.* **116**, 3173 (1994). doi:10.1021/ja00086a077

33. J. Lee *et al*., Nitronyl nitroxide radicals as organic memory elements with both n- and p-type properties. *Angew. Chem. Int. Ed.* **50**, 4414 (2011). doi:10.1002/anie.201004899

34. C. P. Collier *et al*., A [2]catenane-based solid state electronically reconfigurable switch. *Science* **289**, 1172 (2000). doi:10.1126/science.289.5482.1172 Medline

35. J. E. Green *et al*., A 160-kilobit molecular electronic memory patterned at 10(11) bits per square centimetre. *Nature* **445**, 414 (2007). doi:10.1038/nature05462 Medline

36. H. Usta, A. Facchetti, T. J. Marks, n-Channel semiconductor materials design for organic complementary circuits. *Acc. Chem. Res.* **44**, 501 (2011). doi:10.1021/ar200006r Medline

37. K. Nakahara, K. Oyaizu, H. Nishide, Organic radical battery approaching practical use. *Chem. Lett.* **40**, 222 (2011). doi:10.1246/cl.2011.222

38. D. J. Williams *et al*., Molecular Meccano. 4. The self-assembly of [2]catenanes incorporating photoactive π-extended systems. *J. Am. Chem. Soc.* **117**, 11171 (1995). doi:10.1021/ja00150a015

39. G. M. Sheldrick, SHELXTL Version 6.14; Bruker Analytical X-ray Instruments, Inc.: Madison, WI (2003).

40. S. Blundell, *Magnetism in Condensed Matter* (Oxford Univ. Press, New York, 2001).

41. R. Krishnan, J. S. Binkley, R. Seeger, J. A. Pople, Self-consistent molecular orbital methods. XX. A basis set for correlated wave functions. *J. Chem. Phys.* **72**, 650 (1980). doi:10.1063/1.438955

42. M. J. Frisch, J. A. Pople, J. S. Binkley, Self-consistent molecular orbital methods 25: Supplementary functions for Gaussian basis sets. *J. Chem. Phys.* **80**, 3265 (1984). doi:10.1063/1.447079

43. D. J. Tannor *et al*., Accurate first principles calculation of molecular charge distributions and solvation energies from ab initio quantum mechanics and continuum dielectric theory. *J. Am. Chem. Soc.* **116**, 11875 (1994). doi:10.1021/ja00105a030